

1 **Observation of the Transport and Removal of Lipofuscin from the Mouse Myocardium**
2 **using Transmission Electron Microscope**

3

4 Lei Wang⁴, Chang-Yi Xiao^{1,2,3,4*}, Jia-Hua Li⁴, Gui-Cheng Tang⁴, Shuo-Shuang Xiao⁴

5 1. Key Laboratory of Ischemic Cardiovascular and Cerebrovascular Diseases Translational
6 Medicine (Three Gorges University), Yichang, Hubei 443003, China

7 2. Central Laboratory, Yichang Central People's Hospital, Yichang, Hubei 443003, China

8 3. Central Laboratory, First Clinical Medical College, China Three Gorges University

9 4. Medical college, China Three Gorges University, Yichang 443002, China

10

11 Lei Wang: wlstones1978@126.com

12 Chang-Yi Xiao: xiaochy@ctgu.edu.cn

13 Jia-Hua Li: lijiahua62@163.com

14 Gui-Cheng Tang: tangguich@126.com

15 Shuo-Shuang Xiao: xiaoshsh@163.com

16

17

18

19

* Corresponding author, xiaochy@ctgu.edu.cn

21 **Abstract:**

22 This study was performed to investigate whether the lipofuscin formed within cardiomyocytes
23 can be excluded by the myocardial tissue. We have provided indicators that can be used for
24 future studies on anti-aging interventions.

25 In the present study, the heart of a 5-month-old BALB/c mouse was obtained for resin
26 embedding and ultra-thin sectioning. The specimens were observed under a Hitach 7500
27 transmission electron microscope, and the images were acquired using an XR401
28 side-insertion device.

29 Lipofuscin granules are found abundantly in myocardial cells. Cardiomyocytes can excrete
30 lipofuscin granules into the myocardial interstitium using capsule-like protrusions that are
31 formed on the sarcolemma. These granules enter the myocardial interstitium and can be
32 de-aggregated to form "membrane-like garbage", which can pass from the myocardial stroma
33 into the lumen of the vessel through its walls in the form of soluble fine particles through
34 diffusion or endocytosis of capillaries. Smaller lipofuscin granules can pass through the walls
35 of the vessels and enter the blood vessel lumen through the active transport function of the
36 capillary endothelial cells. When the extended cytoplasmic end of macrophages and
37 fibroblasts fuse with the endothelial cells, the lipofuscin granules or clumps found in the cells
38 of the myocardial interstitium are transported to the capillary walls, and then, they are
39 released into the lumen of the blood vessel by the endothelial cells.

40 The myocardial tissues of mice have the ability to eliminate the lipofuscin produced in the
41 cardiomyocytes into the myocardial blood circulation. Although there are several mechanisms
42 through which the myocardial tissues release lipofuscin into the bloodstream, it is mainly
43 carried out in the form of small, fine, soluble, continuous transport.

44

45 Key words: lipofuscin; myocardium; mice; exclusion; transport

46

47 **Introduction**

48 It is well known that one of most important research areas in *in vivo* anti-aging intervention is
49 to discover objective evaluation indicators. The content of lipofuscin in organs is an important
50 indicator for assessing the aging status. Lipofuscin is a yellowish-brown pigment composed
51 of highly oxidized proteins, lipids, and metals. Lipofuscin is widely observed in post-mitotic
52 cells, especially in cells with long life spans such as neurons and cardiomyocytes[1,2].
53 Lipofuscin is often known as the "age pigment" and is considered a hallmark of aging. This is

54 not only because the amount of lipofuscin increases with age, showing an approximately
55 linear dependence, but also, and more importantly, because the rate of lipofuscin
56 accumulation correlates negatively with longevity[3-7].

57 Lipofuscin, or age pigment, represents an intra-lysosomal polymeric material that cannot be
58 degraded by lysosomal hydrolases. Although its continuous accumulation over time in
59 post-mitotic cells, such as neurons and cardiomyocytes, has been known for more than 100
60 years, it has recently been suggested that accumulated lipofuscin may be hazardous to cellular
61 functions[6, 8, 9]. There are strong indications that progressive deposition of lipofuscin
62 ultimately decreases cellular adaptability and promotes the development of age-related
63 pathologies, including neuro-degenerative diseases, heart failure, and macular degeneration[8,
64 9]. von Zglinicki T *et al.* found that accelerated lipofuscin accumulation is sufficient to block
65 cellular proliferation within a short period time and induce cell death. They concluded that
66 accumulation of lipofuscin in post-mitotic cells is not just a harmless consequence of ageing,
67 but rather one of the most important causes of senescence[10].

68 Some researchers believe that the accumulation of lipofuscin within post-mitotic cells occurs
69 primarily because it is non-degradable and cannot be removed from the cells through
70 exocytosis[11, 12].

71 However, previous studies have shown that lipofuscin might be released from tissues or cells.
72 A study by El-Ghazzawi *et al.* strongly suggested that nerve cells physiologically remove
73 lipofuscin into the capillary endothelium[13]. Upon treatment with meclofenoxate, there is a
74 gradual decrease in the volume of the pigment in the myocardium. After a treatment period of
75 4-6 weeks, the pigment bodies were found to be lodged in the capillary endothelium and the
76 lumen, which facilitates the removal of the pigment through the blood stream[14]. Joris *et al.*
77 observed the formation and outcome of lipofuscin in human coronary endothelium, and
78 showed that the bulging cell processes containing lipofuscin probably eventually break off
79 and are shed into the bloodstream[15]. Similarly, it has also been proposed that neuronal
80 lipofuscin was transported to the capillary wall and extruded into the lumen in the avian
81 brain[16]. However, some researchers have questioned the studies showing the exclusion of
82 lipofuscin from tissues[17].

83 Hence, it is still not conclusive whether the non-dividing cells in tissues and organs possess a
84 mechanism for excluding lipofuscin. To ascertain whether the heart has a mechanism for
85 eliminating lipofuscin from the myocardium, we carried out investigations using the mouse
86 heart.

87

88 **1. Materials and Methods**

89 Five-month-old BALB/c mice were purchased from Laboratory Animal Center of our
90 institution. All applicable international, national and institutional guidelines for the care and
91 use of animals were followed. The animals were anesthetized using ether. The chest was
92 opened and the heart was removed. Small tissue blocks were obtained from the anterior wall
93 of the left ventricle and were fixed with 1.5% glutaraldehyde. The fixed tissue blocks were
94 further treated with 1% osmium tetroxide, dehydrated, and embedded in epoxy resin. The
95 specimens were sliced using the Microm HM340E rotary ultramicrotome produced by Leica
96 Microsystems Heidelberg GmbH in Germany, and the ultra-thin sections were placed on a
97 copper screen and stained again using lead nitrate and uranyl acetate. Finally, specimens were
98 observed with a Hitachi 7500 transmission electron microscope, and images were acquired
99 using an AMT XR401 side insertion drawing equipment produced by Advanced Microscopy
100 Techniques in USA.

101

102 **2. Results**

103 **2.1. Myocardial fibers (Cardiac cells)**

104 Microscopic observation of myocardial tissue revealed clearly visible lipofuscin deposits that
105 were scattered around the myocardial fibers (cardiac cells) and myocardial interstitium. These
106 lipid-containing, brown deposits were granular or agglomerated; widely varied in size and
107 form; displayed high or medium electron density; uniform or uneven internal structure; or
108 lamellar or lipid droplets; with or without membrane coating; or dispersed or aggregated into
109 large clumps.

110 Lipofuscin found in the myocardial fibers was mainly distributed in the cytoplasm-rich
111 regions at both ends of the nucleus and was interspersed between a large numbers of
112 mitochondria. The distribution of lipofuscin granules was lower in the myofibrils that were far
113 from the nucleus (Fig 1). Lipofuscin granules could also be seen at the edges of myocardial
114 fibers and below the sarcolemma (Fig 2, 15, 16).

115 **Fig 1. Longitudinal section of myocardial fiber in mouse heart.**

116 In the vertical axis of the myocardial fiber in the figure, an oval-shaped cell nucleus can be seen. A large number
117 of densely arranged mitochondria can be seen in the cytoplasm at both ends of the nucleus, and there are
118 multiple lipofuscin granules with high electron density among the mitochondria. These lipofuscin granules are of
119 different sizes and uneven internal structures. Several scattered lipofuscin granules can also be seen among the
120 myofibrils (shown by black arrows). ($\times 15000$, scale plate: 2 μm)

121 **Fig 2. Myocardial fibers and capillary in mouse heart.**

122 Three lipofuscin granules with high electron density can be seen within the myocardial fiber in the right half of
123 the picture close to the capillary wall. They protrude from the surface of the myocardial fiber covered only by a
124 layer of sarcolemma (shown by black arrows). There is no basement membrane outside the capillary
125 endothelium. In the deeper part of the myocardial fiber, two lipofuscin-like granules with different electron
126 densities can be seen (shown by white arrows). ($\times 15000$, scale plate: 1 μm)

127

128 Compared with the lipofuscin granules located deep in the cardiomyocytes, the granules
129 located around the cardiomyocytes were significantly smaller. The sarcolemma on the surface
130 of cardiomyocytes was clearly visible, but often displayed unevenness. Bulging, rod-, sac-, or
131 capsule-like protrusions of different sizes and lengths, were often observed, which contained
132 the lipofuscin granules (Fig 3, 4, 9, 13).

133 **Fig 3. Myocardial fiber and capillary in mouse heart.**

134 The right-hand side of the figure shows a partial longitudinal cut of a myocardial fiber. A capsule-like protrusion
135 can be seen on the surface of the myocardial fiber (shown by a white thick arrow). In the inner center of the top
136 of the capsule-like protrusion, a high electron density spherical lipofuscin granule can be seen. A lipofuscin
137 granule similar to that present in the protrusion can also be seen inside the myocardial fibers near the site where
138 the capsule-like protrusion exits (shown by a black arrow). The capillary endothelium is continuous and intact,
139 and its cytoplasm contains numerous vesicles. The basement membrane outside the endothelium is thin and
140 discontinuous. There are two fibroblast terminal cytoplasmic fragments attached to the upper part outside the
141 capillary wall (shown by white thin arrows). ($\times 20000$, scale plate: 800 nm)

142 **Fig 4. Myocardial fiber and myocardial interstitium in mouse heart.**

143 This image shows a longitudinal section of the myocardial fiber. A narrow gap can be seen between the two
144 myocardial fibers. The sarcolemma on the surface of the myocardial fiber on the left side of the gap is clearly
145 visible, and the walking is smooth. The surface of the myocardial fiber on the right side of the gap is uneven, and
146 there are several capsule-like protrusions on the surface of the myocardial fiber (shown by black arrows) of
147 different sizes, heights, and widths. In the middle region of the cytoplasm inside the larger protrusion, there are
148 several lipofuscin granules with high electron density. ($\times 20000$, scale plate: 800 nm)

149

150 **2.2. Cells in myocardial interstitium**

151 In addition to being rich in capillaries, the interstitial space between myocardial fibers also
152 had two types of cells, fibroblasts and macrophages, with fibroblasts being the predominant
153 type.

154 Fibroblasts are slender spindle-shaped cells and their cell bodies extend along the longitudinal
155 direction of the myocardial fibers with both their ends stretching far. The surface of fibroblast
156 is smooth with no visible phagocytosis. Fibroblasts have a dense cytoplasmic structure and
157 abundant organelles, which contain abundant rough endoplasmic reticulum, free ribosomes,

158 and mitochondria (Fig 5, 6, 7, S1 Fig).

159 **Fig 5. Myocardial interstitium of mouse heart.**

160 Arranged from the top to the bottom in the cardiac interstitium, a fibroblast (shown by a white arrow), a
161 macrophage (shown by a black arrow), and capillary. The fibroblast has a high density of organelles in the
162 cytoplasm, with abundant rough endoplasmic reticulum, free ribosomes, and mitochondria. The macrophage has
163 relatively low cytoplasmic density, rich cytoplasm, abundant vesicles including phagocytic vesicles, and more
164 lipid-like lipofuscin masses. These lipofuscin masses differ in size, internal structure, and electron density. The
165 macrophage is closely attached to the capillary below, and the basement membrane outside the capillary in this
166 area is incomplete or even missing. ($\times 10\,000$, scale plate: $1\ \mu\text{m}$)

167 **Fig 6. Fibroblast in myocardial interstitium of mouse heart.**

168 A fibroblast is long spindle-shaped cell that is present in the longitudinal direction of the myocardial fibers with
169 slender ends. The cytoplasm has high density and is rich in organelles. It also contains lipofuscin granules or
170 clumps of varying sizes. These lipofuscinous granules or clumps have uneven internal structures and different
171 morphologies, have high electron density, and have no membrane coating on the periphery. ($\times 12\,000$, scale plate:
172 $1\ \mu\text{m}$)

173 **Fig 7. Myocardial tissue around extracellular space in mouse cardiac myocardium.** In the myocardial tissue
174 around the extracellular space, a layer of cells is often visible on the surface of the myocardial fibers. This layer
175 of cells can have different cellular characteristics, such as fibroblastic type (shown by the white arrow) or
176 phagocytic type (shown by the black arrow). In addition to rich organelles, the cytoplasm of these cells will
177 contain some lipofuscin-like mass or granules with high or medium electron density. Most of the lipofuscin
178 granules are found within the phagocytic cell. ($\times 20\,000$, scale plate: $800\ \text{nm}$)

179
180 In addition, they also contain a large number of lipofuscin granules or clumps of varying sizes
181 and shapes. The elongated cytoplasmic ends of the fibroblasts contain the lipofuscin granules
182 or clumps, which can adhere to the capillaries and fall off. The structural density of the shed
183 cytoplasm at the end of fibroblasts is higher, with higher electron density, and often has
184 structural characteristics that are similar to lipofuscin (Fig 6, 7, 8, and S1, S2 Figs). The
185 basement membrane outside the capillary vessel wall, which is in close contact with the
186 cytoplasm of fibroblasts, often disappears, such that the shed cytoplasm can directly adhere to
187 and fuse with the endothelial cells.

188 **Fig 8. Capillary and perivascular tissue between myocardial fibers in mouse heart.**

189 In the interstitial space between the capillary and myocardial fibers, a large amount of messy substance can be
190 seen, some are solid cluster-like structures (shown with white arrows), and some are "membrane-like garbage"
191 (shown with black arrows). The solid clusters have high electron density, an uneven internal structure, and are
192 composed of amorphous substances, which are most likely the cytoplasmic fragments of a fibroblast. The
193 "membrane-like garbage" has a medium electron density, and can form a single layer or multiple layers with
194 irregular structure in size, density and morphology, and partly form lamellar myelin figure structures. The
195 sac-like structures made of these "membrane-like garbage" are all far away from the capillary and close to the
196 myocardial fiber. ($\times 20\,000$, scale plate: $800\ \text{nm}$)

197

198 Macrophages are primarily oblong in shape and possess rough surface with several wrinkles
199 or protrusions of different sizes, visibly exhibiting swallowing, phagocytosing and
200 encapsulation of large granules. The internal structure of the cytoplasm is relatively loose and
201 contains abundant vesicles, phagocytosed particles, and higher number of lipid droplet-like
202 lipofuscin granules. These lipofuscin granules vary widely in size, internal structure, and
203 electron density (Fig 5, 7, 9).

204 **Fig 9. A lipofuscin-containing phagocytic cell in the extracellular space of mouse cardiac myocardium.**

205 The image shows a lipofuscin-containing phagocyte in the myocardial space with the morphological
206 characteristics of macrophages. The cell surface is not smooth and has many wrinkles or protrusions of various
207 sizes. There are visible signs of wrapping and swallowing. The cell contains multiple lipofuscin particles and
208 lumps of various sizes, which have higher electron density. Parts of the lipofuscin granules have uneven internal
209 structures with a large difference in electron density. Some lipofuscin granules have lipid droplet-like
210 morphological characteristics. ($\times 10000$, scale plate: 1 μm)

211

212 Macrophages can either be closely attached to the capillaries through their cell body directly
213 or through the cytoplasm that is elongated and shed. The density of the cytoplasmic fragments
214 shed from the cytoplasmic end of the macrophages is relatively low, and the interior mainly
215 consists of sparse fine particles, vesicles, and lipofuscin granules. The basement membrane
216 outside the capillaries where the macrophages are in close contact with the capillary wall is
217 incomplete or even absent (Fig 5, 10-12). No macrophages were observed in and out of the
218 capillaries or lymphatic vessels.

219 **Fig 10. Myocardial interstitium and capillary in mouse heart.**

220 A large number of irregular sacs composed of "membrane-like garbage" can be seen in the myocardial
221 interstitium, which have medium electron density and constitute single or multi-layer irregular sac-like structures
222 with large differences in size, density, and morphology. Some membranous substances are densely formed into
223 lamellar myelin figure structures. Some myelin figure structures are close to the capillary wall, there is no
224 basement membrane with the endothelial cell, and even adheres to the endothelial cell (shown by a black arrow).
225 Similar "membrane-like garbage" can be seen in the capillary cavity. On upper part of the capillary wall,
226 oriented toward the membranous myelinfigure structures gathered, there is no basement membrane outside the
227 endothelium. In the endothelium here, two high-density lipofuscin-like granules (shown by thin white arrows)
228 can be seen, and the granule on the right seems to be partially exposed outside the endothelium. In the middle of
229 the surface of the myocardial fiber in the upper right, the surface sarcolemma protrudes into the stroma, forming
230 a rod-like protrusion (shown by a thick white arrow) ($\times 20000$, scale plate: 800 nm)

231 **Fig 11. Capillary and surrounding tissue in myocardial interstitium of mouse heart.**

232 The central part of the picture is a complete capillary, and the lumen is filled with red blood cells. The vessel
233 wall is surrounded by two endothelial cells, and at the junction of two endothelial cells, tight junctions are
234 formed. In the cytoplasm of endothelial cells of the wall, vesicles are extremely abundant. Most of the

235 endothelium does not have a basement membrane. The endothelium is directly exposed to the interstitial matrix
236 of the myocardium, and is in direct contact with fibers, vesicles, and even myocardial fibers around the
237 capillaries. Slightly above the middle of the left wall of the capillary, a small vesicle can be seen embedded in
238 the endothelium of the capillary wall (shown by a white arrow). In the interstitium above the capillary, a
239 triangular cytoplasmic structure containing several lipofuscin granules can be seen, which is close to the wall of
240 the vessel, and it should be part of the cytoplasmic structure of the lipofuscin-loaded cell in the myocardial
241 interstitial. The lower left side of the cytoplasmic structure is closely attached to the capillary endothelium, and
242 the two parts of the structures seem to be fused (shown by a black arrow). ($\times 20000$, scale plate: 800 nm)

243 **Fig 12. Capillary and outer structure of the vessel wall in the mouse heart myocardium.**

244 In the center of the figure is a complete capillary, the vessel wall is surrounded by two endothelial cells. At the
245 junction of two endothelial cells, tight junctions are formed. The cytoplasmic vesicles of endothelial cells
246 constituting the vessel wall are abundant. There is a continuous and complete basement membrane outside the
247 endothelium of the capillary wall. Outside the endothelial wall of the left and upper capillary, each is covered by
248 one non-endothelial cell structure containing lipofuscin-like matter. There is no basement membrane between the
249 non-endothelial cytoplasmic structure located outside the capillary wall and the endothelial cells, and it is closely
250 attached to the capillary endothelium downward, and the two cell structures seem to be fused (shown by a black
251 arrow). The white arrow shows a mitochondrion inside the non-endothelial cell outside the vessel wall. ($\times 20000$,
252 scaleplate 800nm)

253

254 **2.3. Matrix in myocardial interstitium**

255 In the interstitial matrix of the myocardial space, a large number of non-cellular structured
256 membrane-like structures can be seen, which can be of different sizes and electron density.
257 They form loose, irregular sac-like structures with single or several layers, or dense myelin
258 figures with multiple layers, creating complex structures that greatly vary in size, density,
259 morphology and number of membrane layers (Fig 6, 8, 10-14). We termed these complex
260 membrane-like structures as "membrane-like garbage". These "membrane-like garbage" are
261 widely and irregularly distributed in the matrix of the myocardial interstitium, either sparsely
262 or densely.

263 **Fig 13. Myocardial fibers and interstitium between myocardial fibers in mouse heart.**

264 The image shows the longitudinal section of the myocardial fibers. Wider space is seen between the two
265 myocardial fibers. A large number of randomly distributed "membrane-like garbage" can be seen in the space.
266 These "membrane-like garbage" may form loose, irregular sac-like structures, or densely-formed myelin figure
267 structures. These structures are either loose or dense, with different sizes and shapes, and are scattered in the
268 spaces. The surface of the myocardial fibers on the right side of the space is uneven and the sarcolemma is not
269 very clear. Verruca-like protrusions (shown by white arrow) and several vesicles (shown by black arrows) can be
270 seen on the surface of myocardial fibers. The verruca-like protrusions are broad at the top and slender at the base.
271 A high electron density lipofuscin-like pellet can be seen in the center of the top, and the pellet is surrounded by
272 a thick lipid membrane-like structure. A large lipofuscin mass can be seen deep in the right muscle fiber, with

273 high electron density and uneven internal structure. ($\times 20000$, scale plate: 800 nm)

274 **Fig 14. Myocardial fibers and a capillary in the mouse heart myocardium.**

275 The center of the figure shows a capillary. The thickness of the endothelial cells constituting the vessel wall
276 varies greatly; the cytoplasm contains abundant vesicles and greater number of pellets or particles with high
277 electron density (shown by black arrows). The cytoplasm of the endothelial cells on the left wall has two mini
278 finger-like protrusions (shown by white thin arrows) that extend to the lumen. In addition to red blood cells, the
279 lumen contains a large number of irregularly shaped "membrane-like garbage" that has large differences in size,
280 density, and shape. Densely structured sacs can form lamellar myelin figure structures. "membrane-like garbage"
281 can also be seen in the stroma outside of the capillary (shown by the white thick arrows). ($\times 10000$, scale plate: 1
282 μm)

283

284 In the interstitium, some free lipofuscin particles can also be seen that vary widely in size.
285 Some are in the form of small granules, while others form large masses, which might be either
286 coated or uncoated at the periphery (Fig 14). Large clumps formed by the aggregation of
287 several lipofuscin granules are sometimes seen (Fig 15). Some lipofuscin granules have low
288 density and a relatively loose structure. The shape is similar to the high-density
289 "membrane-like garbage," and there is no obvious morphological boundary as that seen in the
290 "membrane garbage," which is denser in structure (Fig 10-14).

291 **Fig 15. Lipofuscin mass in myocardium of mouse heart.**

292 In the interstitium between myocardial fiber and capillary (or lymphatic vessel), there is a large lipofuscin mass.
293 On the periphery of this huge lipofuscinous mass, intermittent membrane wrapping can be seen only in the area
294 below it. Most part of the lipofuscinous mass is directly exposed in the interstitium, directly with the left
295 myocardial fiber and the capillary (or lymphatic vessel) on the right are attached. The basement membrane is not
296 noticeable between the lipofuscin mass and capillary endothelium (shown by black arrows). At the bottom, there
297 are two separate lipofuscin granules, which are located below the sarcolemma of the myocardial fiber (shown by
298 white arrow). ($\times 15000$, scale plate: 1 μm)

299

300 **2.4. Capillaries in myocardial interstitium**

301 There are many capillaries in the myocardial interstitium, which are continuous in nature.
302 These capillaries can be roughly divided into two types: high density and low density
303 endothelial cell types.

304 High-density endothelial cell-type capillary vessels have thick walls and high cytoplasmic
305 density. Endothelial cells can form tight junctions. In addition to the scattered mitochondria
306 inside the cytoplasm of the endothelial cells, they contain abundant pinocytotic vesicles and
307 exocytosis vesicles. These vesicles are often highly dense, indicating that active transport
308 occurs through their walls. High electron density granules and fine particles are found

309 abundantly in the cytoplasm (Fig 2, 3, 5, 8, 10-12, 16, and S1 Fig).

310 **Fig 16. Two capillaries in mouse heart myocardium.**

311 The endothelial cytoplasm of the right capillary is rich in vesicles and fine particles with high electron density,
312 which makes the tube wall denser. Several scattered lipofuscin granules (shown by the thick white arrows) can
313 be seen in the cytoplasm. There are fewer intracellular vesicles and high electron density particles in the left
314 capillary endothelium. The structure in the tube wall appears loose, but there are scattered lipofuscin particles
315 (shown by the thin white arrows). On the inner side of the upper part of the left vessel wall of this capillary, the
316 cytoplasm of endothelial cell forms several fine finger-like protrusions that penetrate into the lumen, and fall off.
317 There are several cytoplasmic structures outside the tube wall that are close to the endothelial cells, which shows
318 cytoplasmic fusion (shown by black arrows). (×8000, scale plate: 2 μm)

319

320 The walls of low-density endothelial cell-type capillaries are thinner with relatively less dense
321 cytoplasm. The number of vesicles is low, and few large vesicles and slender membrane
322 tubules can also be seen. The cytoplasm contains many small particles with medium to high
323 electron density, which can adhere to the membrane tube, with morphology similar to the
324 rough endoplasmic reticulum (Fig 14, 16, and S2 Fig).

325 Morphologically, these two types of capillaries do not have clear boundaries, and the
326 morphology of some vessels is somewhere in between. The endothelial cell membrane on the
327 lumen side of most capillaries has small conical or tiny finger-like protrusions that are of
328 different lengths and can be extruded into the lumen (Fig 2, 14, 16, and S1, S2 Figs). The
329 cytoplasm of some endothelial cells are embedded with lipofuscin-like granules of different
330 sizes and shapes (Fig 9, 10, 14, 16, and S2 Fig). Occasionally, these granules are embedded
331 into the endothelial cells of the vessel walls from the exterior of the vessel without any
332 basement membrane (Fig 10, 11, and S2 Fig). It can also be seen that the lipofuscin granules
333 in the myelin figure are extruded by the endothelial cells into the lumen from the walls of the
334 vessels (Fig 17).

335 **Fig 17. Capillary in the cardiac myocardium of mouse heart.**

336 In this picture, a capillary can be seen with a high electron density myelin figure lipofuscin mass protruding from
337 the inside of the vessel wall into the lumen at the center of the right vessel wall. (×20000, scale plate: 800 nm)

338

339 "Membrane-like garbage" similar to that found in the myocardial stroma were seen within the
340 lumen of some of the capillaries, which forms sac-like structures formed in the capillary
341 cavity that is more loose and fragmented than the membrane-like garbage formed in the
342 myocardial matrix. The amount of membrane-like garbage in the lumen varies between
343 different blood vessels, and sometimes, there are very obvious differences between the two
344 accompanying blood vessels (Fig 2, 3, 5, 8, 10-12, 14, 16, and S1, S2 Figs). In general, the

345 lumens of the low-density endothelial-type capillaries contain significantly higher amount of
346 membrane-like garbage than the high-density endothelial-type capillaries. This might be
347 because the high-density endothelial-type capillaries are arterial-end capillaries, while
348 low-density endothelial-type capillaries are venous-end capillaries. The blood flowing in the
349 capillaries at the venous end collects more lipofuscin-like substances that are discharged from
350 the capillary walls.

351 Capillary vessels are often surrounded by cell bodies or cytoplasmic fragments of different
352 cell types, which can even be directly attached to the vessel wall. The areas where the
353 extravessel cell body or cytoplasmic fragment is in contact with the capillary vessel wall, the
354 basement membrane is often incomplete or even disappears, resulting in direct contact
355 between the extravessel cytoplasm with the endothelial cells, which leads to blurring of the
356 boundaries between them, and even merging. Extravessel cytoplasmic fragments often contain
357 lipofuscin granules (Fig 5, 10-12, and S1, S2 Figs), or are in a highly dense formation (Fig 3,
358 8, 16, and S1, S2 Figs).

359 Perivascular cells were not observed around the capillaries. All the cytoplasmic fragments that
360 are outside or surround the capillary walls, and even fuse with endothelial cells, are derived
361 from the extended terminal cytoplasm of the macrophages and fibroblasts, or shed
362 cytoplasmic debris.

363

364 **3. Discussion**

365 Do the heart, brain, and retina have the ability to expel the accumulated lipofuscin? Is it
366 possible to speed up the elimination of lipofuscin in these tissues with drugs such as
367 centrophenoxine and meclofenoxate in order to slow down aging? These are some
368 controversial questions[6, 8, 11, 13, 14, 18-20]. Therefore, this study investigates the
369 elimination of lipofuscin from the heart to obtain potential evidence that lipofuscin is excreted
370 by the tissues. These results might facilitate future research on related interventions.

371

372 Observation of myocardial cells revealed that these cells can eliminate lipofuscin. The
373 mechanism of removal of the lipofuscin granules that are located below the sarcolemma
374 might be via the formation of capsule-like protrusions on the sarcolemma and on the
375 sarcoplasm near them, which extend into the interstitial space, detach from the myocardial
376 cells and finally, enter the interstitial space. We did not observe exocytosis of large lipofuscin
377 granules (approximately 1 μm diameter) in the myocardial fibers. This result may indicate

378 that myocardial cells slowly and continuously excrete lipofuscin to the outside in a more
379 subtle way.

380 Most of the lipofuscin particles entering the interstitium will soon disintegrate, de-aggregate,
381 and diffuse, forming "membrane-like garbage" or mini soluble particles, which are dispersed
382 in the interstitial matrix and diffuse around the blood vessels. These particles can enter the
383 vascular wall of the endothelium through simple diffusion, pinocytosis of capillary
384 endothelium, followed by further diffusion into the bloodstream; or be directly released into
385 the bloodstream by exocytosis. Some mini lipofuscin particles can be adsorbed and fused with
386 other membranous structures (lumen cell membrane, tubules, and vesicles) in the cytoplasm.
387 The vesicles and tubules that fuse with lipofuscin will also merge into the surface membrane
388 of endothelial cell lumen. It cannot be excluded that the mini soluble lipofuscin particles that
389 have diffused into the endothelial cells re-aggregate in the endothelial cytoplasm to form
390 larger lipofuscin granules, which are then "pushed" into the lumen by endothelial cells. This is
391 similar to the phenomenon observed by Joris I *et al.* in human coronary artery where it was
392 seen that endothelial lipofuscin is excreted through enlarged cell processes[15]. A few of the
393 smaller undisintegrated lipofuscin granules might be directly embedded into the capillary
394 endothelium in the form of granules, and then enter the lumen in a "pushed" mode.

395
396 Lipofuscin masses in the macrophages might have arisen from three possible ways. First, it
397 might be derived from phagocytosis of intact lipofuscin granules in the matrix. Second, it
398 might be due to micro-engulfing of "membrane-like garbage" along with micro-phagocytosis
399 of fine particles formed by de-aggregation of lipofuscin. These swallowed lipid molecules and
400 phagocytosed particles then aggregate in the cell to form large lipofuscin granules or mass.
401 Third, it might be due to phagocytosis and digestion of other cellular and tissue structural
402 fragments in the cardiac interstitium. The lipofuscin formed through these three methods will
403 eventually aggregate in the macrophages, forming huge lipofuscin masses.

404 How do macrophages containing large amounts of lipofuscin transfer lipofuscin away from
405 the myocardial tissue? According to our observations and speculations, one of the most
406 significant ways is to transport lipofuscin into the lumen of the blood vessel through fusion
407 with capillary endothelial cells. Thus, the end of the elongated cytoplasm containing
408 lipofuscin granules is close to the capillaries, and it eventually fuses with endothelial cells
409 releasing the lipofuscin granules into the cytoplasm of endothelial cells. The lipofuscin
410 granules entering the vessel wall are transported by the endothelial cells into the lumen in a
411 "pushed" mode, thereby completing the process of transferring lipofuscin from the extravessel

412 stroma into the lumen (Fig 18).

413 **Fig 18. Schematic diagram of the lipofuscin excretion through the capillaries in the myocardial**
414 **interstitium of the mouse heart.**

415 The figure shows four possible pathways through which the lipofuscin found in the myocardial interstitium
416 enters the capillary cavity. Pathway 1: The lipofuscin granules are close to the capillary wall, and the granules
417 gradually disaggregate to form soluble micro-particles. These microparticles enter the endothelium of capillaries
418 by simple diffusion, and then aggregate in the cytoplasm of the endothelial cells to form fine lipofuscin particles.
419 These particles can adhere and subsequently fuse with the membrane-bound vesicles and tubules in the
420 cytoplasm, as well as the cell membrane on the lumen surface. Membrane vesicles and tubules fused with
421 lipofuscin can further merge with the cell membrane on the lumen surface. The cell membrane of the luminal
422 surface with lipofuscin forms fine finger-like protrusions into the cavity and these protrusions continue to
423 elongate and eventually fall off to enter the blood stream. Pathway 2: The lipofuscin granules swell and dissolve,
424 forming a lamellar membrane-like myelin figure structure, and further disaggregate to form soluble
425 microparticles or lipid molecules, which can re-aggregate in the interstitium to form irregular membrane sacs, or
426 they can diffuse directly through the basement membrane. Irregular membrane sacs formed by re-aggregation in
427 the interstitium will soon disaggregate to form soluble microparticles or lipid molecules that can diffuse through
428 the basement membrane and enter the capillary lumen directly through simple diffusion, or they can be
429 swallowed by the endothelium to form pinocytotic vesicles, which are transferred into the cavity. Finally, these
430 micro-particles and lipid molecules are expelled into the lumen by exocytosis where they can re-aggregate. In the
431 circulating plasma, they aggregate again to form membrane vesicles of different sizes and shapes. Pathway 3:
432 Lipofuscin granules in the interstitium enter the fibroblast cells or macrophages, and these cells can extend their
433 lipofuscin-containing cytoplasm to the capillary and closely adhere to the vessel wall. The protruding
434 cytoplasmic portion containing lipofuscin granules can get detached from the original cell body. The basement
435 membrane outside the endothelium of the capillary wall that is attached to the cytoplasm of lipofuscin-containing
436 cell disappears, and the two cells closely adhere. Finally, these cells are fused, and the lipofuscin-containing cell
437 cytoplasm merges with the endothelium. Simultaneously, the lipofuscin granules that are brought into the
438 endothelial cells can be "pushed" into the capillaries. Pathway 4: Lipofuscin granules pass through the basement
439 membrane, directly enter the capillary endothelium, and then are extruded into the lumen of the blood vessel in a
440 "pushed" manner. They finally fall off from the endothelium to enter the blood stream where they rapidly swell
441 and disintegrate to form lamellar myelin figure structures with a relatively loose structure, and further
442 disaggregate to form "membrane-like garbage".

443

444 The lipofuscin mass present in the fibroblasts might exist due to two reasons; one is due to the
445 production of its own cell metabolism and the other is due to microphagocytosis, similar to
446 the macrophages. Previous studies have shown that fibroblasts in the myocardial tissue
447 possess a certain phagocytic function[10, 21]. However, in the present study, we did not
448 observe engulfment of lipofuscin granules by the fibroblasts. Fibroblasts also seem to have
449 the ability to excrete lipofuscin and similar to that seen in macrophages, it is excreted into
450 blood vessels by fusion with capillary endothelial cells. Thus, the elongated cytoplasmic ends

451 containing lipofuscin granules is close to the capillaries and fuses with endothelial cells,
452 which releases the lipofuscin material into the cytoplasm of endothelial cells, and finally into
453 their lumen in a "pushed" manner.

454 As the myocardial tissues we observed are located in the deeper regions of the heart wall,
455 only capillaries that extend between the myocardial fibers, close to the myocardial fibers were
456 visualized, along with a few connective tissues. Therefore, the pericytes or mast cells that
457 were described by other researchers were not observed around the capillaries in our
458 specimens[22].

459 Comparison of the amount of "membrane-like garbage" in different capillary lumens showed
460 that myocardial tissues "dump" a large amount of "garbage" into the bloodstream during the
461 blood flow, which is mainly derived from lipofuscin produced from myocardial cells, and this
462 dumping is not slow. According to our observations, there are several modes of transport of
463 lipofuscin in the myocardium through the capillary wall (Fig 18). Although there are many
464 modes of transfer, the in-wall and out-wall modes of these transfers are not a fixed
465 combination, and there can be different combinations between different in-wall and out-wall
466 modes. However, from the frequency shown by various transport modes, the cross-wall
467 transport of lipofuscin in myocardial tissue may mainly rely on a small, fine, soluble,
468 continuous transport mode, it is not a one-time, massive, or cell-carrying transfer. This small,
469 fine, soluble, continuous transport pattern is slightly similar to the lipofuscin elimination
470 phenomenon observed in the seminiferous tubules of animal testes[23,24].

471 Many previous studies have described the presence of lymphatic vessels in the myocardium
472 [25]. However, in the current study, lymphatic vessels with typical structural features were not
473 observed. It is therefore uncertain whether a lipofuscin excretion pathway through the
474 lymphatic vessels exists. This is completely different from the case where the lipofuscin
475 discharged directly into the lymphatic ducts is observed in the testicular seminiferous
476 tubules[23,24].

477 In this study, we observed that some of the lipofuscin particles were transferred within the
478 myocardial tissue; and across the capillary wall into the blood flow. However, there are still
479 some unanswered questions, such as, is lipofuscin mainly transported in a soluble manner in
480 the myocardium[26]? Is it possible to remove the lipofuscin present in the form of huge
481 clumps? How is it cleared? What roles do fibroblasts play in the elimination of lipofuscin in
482 the myocardium? Do the myocardial tissues from different parts of the mice heart treat
483 lipofuscin in the same way? Further investigations are needed to answer these questions.

484

485 **Supporting information**

486 **S1 Fig. Capillary and fibroblast in the cardiac myocardium of mouse heart.**

487 A complete capillary can be seen in the myocardial interstitium. The lumen of the capillary is almost filled
488 with red blood cells, leaving a little space on the top. There are several elongated finger-like protrusions
489 from the endothelial cell. Below the capillary, a fibroblast can be seen, with an elongated protrusion, and it
490 is closely attached to the outer wall of the capillary. In this area, there is no basement membrane noticeable,
491 and thus, the end of the protrusion is directly attached to the endothelial cell (shown by black arrows).
492 Above the capillary, there are two small lipofuscin-like granules (shown by white arrows). ($\times 20000$, scale
493 plate: 800 nm) (shown by thin white arrows)

494 **S2 Fig. Structure of a capillary in the myocardium of the mouse heart.**

495 It can be seen that the capillary wall is thick, structural density of the endothelial cell is low, and the
496 number of vesicles is low. In the cytoplasm of endothelial cell, three medium-high electron density
497 spherical lipofuscin granules (shown by black arrows), few medium-high electron density fine particles,
498 and several medium-high electron density tubules can be seen. The left inner wall of the capillary is not
499 smooth, and the endothelial cell membrane protrudes into the lumen, forming fine finger-like protrusions
500 and vesicles. Membrane sacs and membrane debris-like structures are scattered throughout the capillary
501 cavity. The exterior of the vessel wall on both sides contains cytoplasmic fragments of extramural cells
502 attached to the exterior of the endothelial cell (shown by white arrows). ($\times 20\ 000$, scale plate: 800 nm)

503

504 **Authors' contributions**

505 Lei Wang performed the morphological observation, animal feeding and sample collection.

506 Chang-Yi Xiao organized or participated in the design of the study and performed the
507 morphological observation.

508 Jia-Hua Li and Gui-Cheng Tang were responsible for the preparatory laboratory work,
509 dissection, and initial preparation and processing of the samples.

510 Xiao Rong-Shuang provided help in modifying the English translation of the manuscript.

511 All authors read and approved the final manuscript.

512

513 **Competing interests:**

514 The authors have declared that no competing interests exist.

515

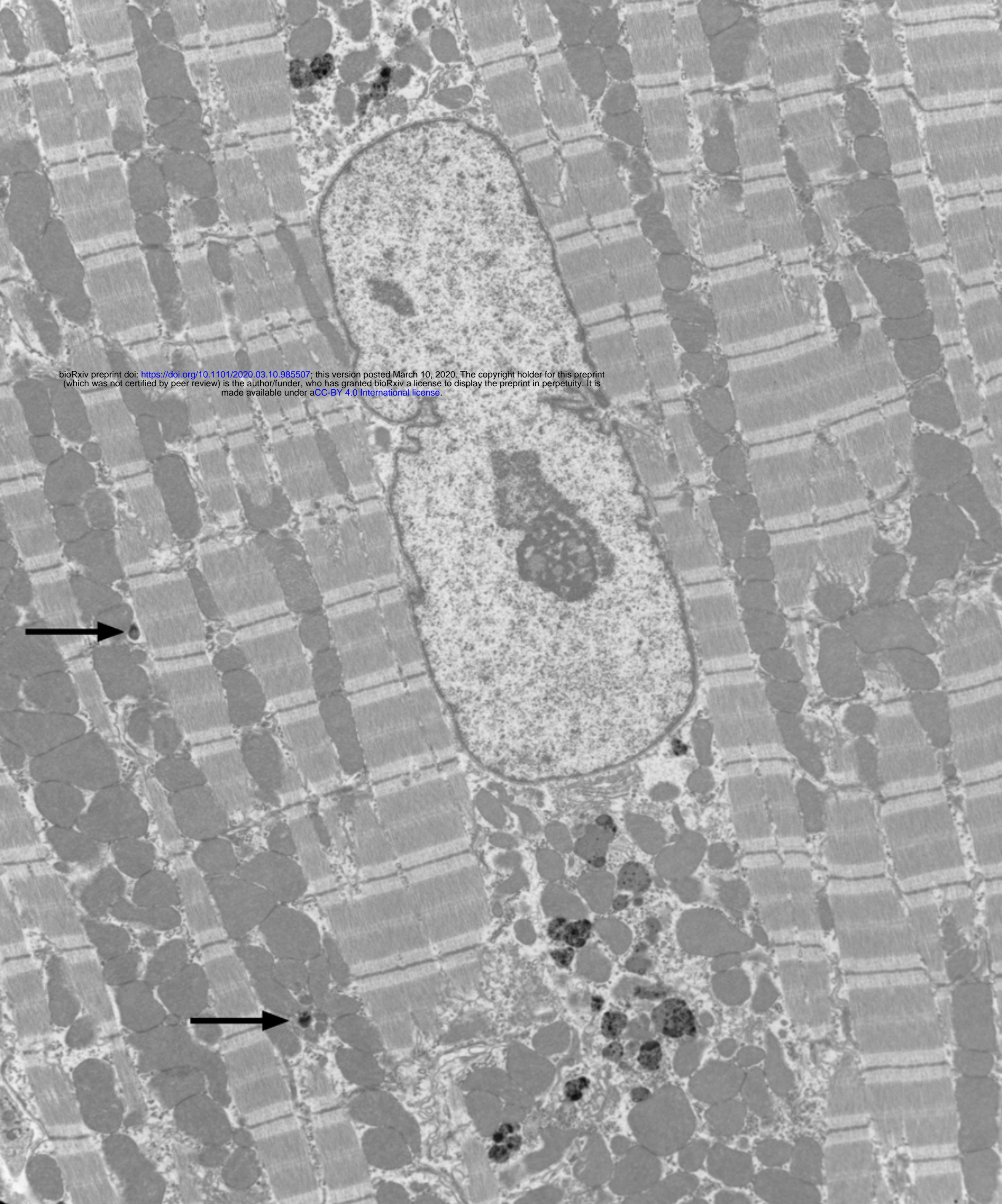
516 **References**

517 1. Kakimoto Y, Okada C, Kawabe N, Sasaki A, Tsukamoto H, Nagao R, et al. Myocardial
518 lipofuscin accumulation in ageing and sudden cardiac death. *Sci Rep.* 2019;9: 3304.

- 519 2. Malkoff DB, Strehler BL. The ultrastructure of isolated and in situ human cardiac age
520 pigment. *J Cell Biol.* 1963;16: 611-6.
- 521 3. Strehler BL, Mark DD, Mildvan AS, Gee MV. Rate of magnitude of age pigment
522 accumulation in the human myocardium. *J. Gerontol.* 1959;14: 430–439.
- 523 4. Munnell JF, Getty R. Rate of accumulation of cardiac lipofuscin in the aging canine. *J*
524 *Gerontol.* 1968;23: 154–158.
- 525 5. Nakano M, Gotoh S. Accumulation of cardiac lipofuscin depends on metabolic rate of
526 mammals. *J Gerontol.* 1992;47: B126–B129.
- 527 6. Brunk UT, Terman A. Lipofuscin: mechanisms of age-related accumulation and influence
528 on cell function. *Free Radic Biol Med.* 2002 Sep 1;33: 611-9.
- 529 7. Porta EA. Pigments in aging: an overview. *Ann N Y Acad Sci.* 2002;959: 57-65.
- 530 8. Terman A, Brunk UT. Lipofuscin. *Int J Biochem Cell Biol.* 2004;36: 1400-4.
- 531 9. Höhn A, Grune T. Lipofuscin: formation, effects and role of macroautophagy. *Redox Biol.*
532 2013;1: 140-144.
- 533 10. von Zglinicki T, Nilsson E, Döcke WD, Brunk UT. Lipofuscin accumulation and ageing
534 of fibroblasts. *Gerontology.* 1995;41 Suppl 2:95-108.
- 535 11. Terman A, Brunk UT. Ceroid/lipofuscin formation in cultured human fibroblasts: the role
536 of oxidative stress and lysosomal proteolysis. *Mech Ageing Dev.* 1998;104: 277-291
- 537 12. Sitte N, Huber M, Grune T, Ladhoff A, Doecke WD, Von Zglinicki T, et al. Proteasome
538 inhibition by lipofuscin/ceroid during postmitotic aging of fibroblasts. *FASEB J.* 2000;14:
539 1490-8.
- 540 13. El-Ghazzawi EF, Malaty HA. Electron microscopic observations on extraneuronal
541 lipofuscin in the monkey brain. *Cell Tissue Res.* 1975;161: 555-65.
- 542 14. Patro N, Sharma SP, Patro LK. Lipofuscin accumulation in ageing myocardium and its
543 removal by meclophenoxate. *Indian J Med Res.* 1992;96: 192–198.
- 544 15. Joris I, Billingham ME, Underwood JM, Majno G. Lipofuscin and lipid oxidation in
545 human coronary endothelium. *Cardiovasc Pathol.* 1998;7: 75-85
- 546 16. Singh R, Mukherjee B. Some observations of the lipofuscin of the avian brain with a
547 review of some rarely considered finding concerning the metabolic and physiologic
548 significance of the neuronal lipofuscin. *Acta Anat.* 1972;83: 302–320.
- 549 17. Katz ML,. Potential reversibility of lipofuscin accumulation. *Arch Gerontol Geriatr.*
550 2002;34: 311-7.
- 551 18. Katz ML,, Rice LM, Gao C. Reversible accumulation of lipofuscin-like inclusions in the
552 retinal pigment epithelium. *Invest Ophthalmol Vis Sci.* 1999;40: 171–181.

- 553 19. Nandy K, Bourne GH. Effect of centrophenoxine on the lipofuscin pigments in the
554 neurones of senile guinea-pigs. *Nature*. 1966;210: 313–314.
- 555 20. Terman A, Brunk UT. On the degradability and exocytosis of ceroid/lipofuscin in cultured
556 rat cardiac myocytes. *Mech Ageing Dev*. 1998;100:145-56.
- 557 21. Elleder M, Drahota Z, Lisa V, Mares V, Mandys V, Muller J, et al. Tissue culture loading
558 test with storage granules from animal models of neuronal ceroid-lipofuscinosis (Batten
559 disease): testing their lysosomal degradability by normal and Batten cells. *Am J Med
560 Genet*. 1995;57: 213–221.
- 561 22. Gersch C, Dewald O, Zoerlein M, Michael LH, Entman ML, Frangogiannis NG. Mast
562 cells and macrophages in normal C57/BL/6 mice. *Histochem Cell Biol*. 2002;118: 41-9.
- 563 23. Xiao C-Y, Wang Y-Q, Li J-H, Tang G-C. Formation and outcome of residual bodies in
564 seminiferous tubules of the mouse testis. *Acta Med Univ Sci Technol Huazhong*. 2016;45:
565 529-34
- 566 24. Xiao C-Y, Wang Y-Q, Li J-H, Tang G-C, Xiao S-S. Transformation, migration and
567 outcome of residual bodies in the seminiferous tubules of the rat testis. *Andrologia*.
568 2017;49: e12786.
- 569 25. Sommer JR, Jennings RB. Ultrastructure of cardiac muscle. In: Fozzard, HA, Haber E,
570 Jennings RB, Katz AM, Morgan HE, editors. *The heart and cardiovascular system*.
571 Volume I. 2nd ed. New York: Raven Press; 1991. pp. 3-50
- 572 26. Jolly RD, Palmer DN, Dalefield RR. The analytical approach to the nature of lipofuscin
573 (age pigment). *Arch Gerontol Geriatr*. 2002;34: 205-17.
- 574

bioRxiv preprint doi: <https://doi.org/10.1101/2020.03.10.985507>; this version posted March 10, 2020. The copyright holder for this preprint (which was not certified by peer review) is the author/funder, who has granted bioRxiv a license to display the preprint in perpetuity. It is made available under aCC-BY 4.0 International license.

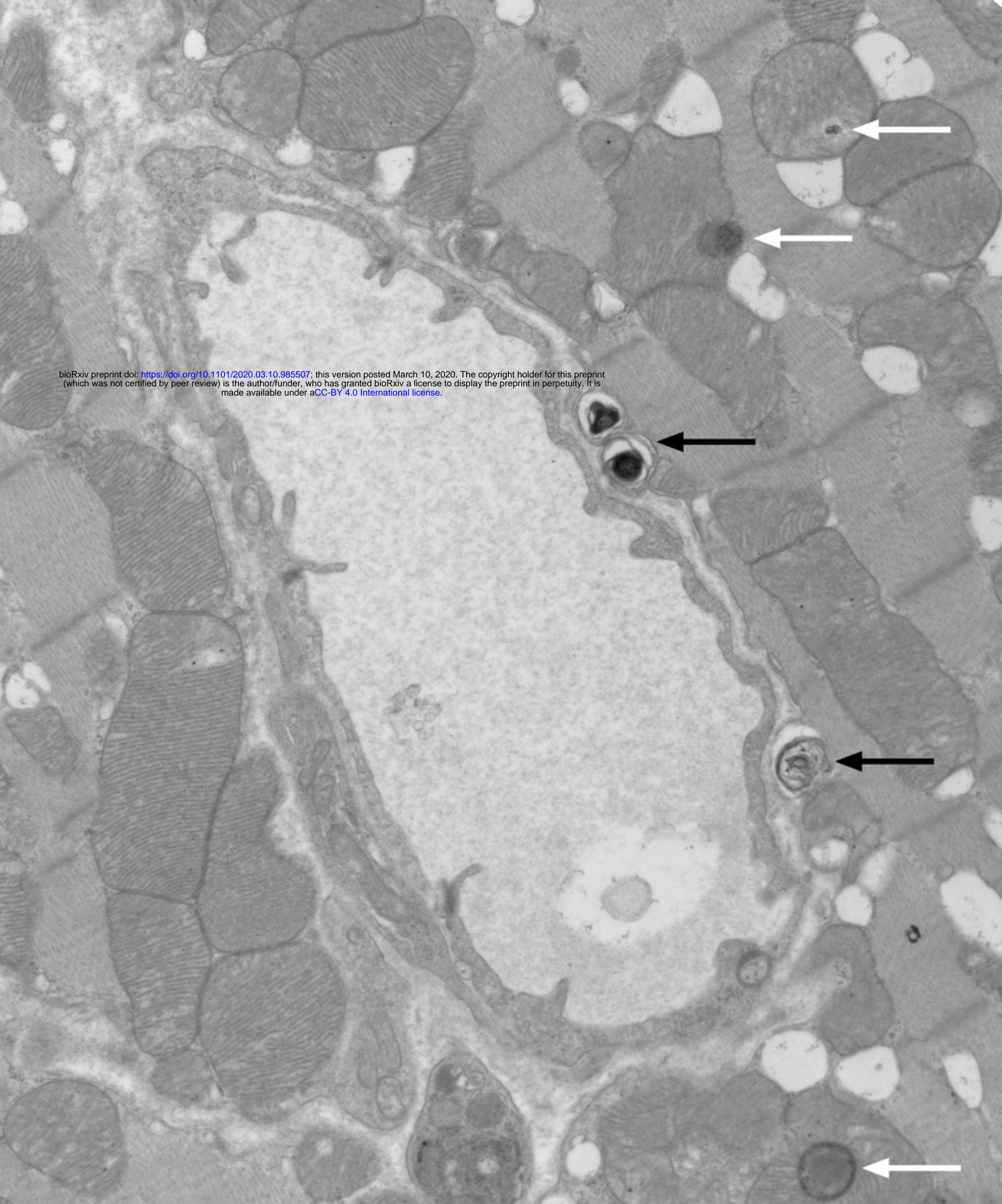


Direct Mag: 7000x
17:26:38 2019/5/9

2 μ m

Figure 1

bioRxiv preprint doi: <https://doi.org/10.1101/2020.03.10.985507>; this version posted March 10, 2020. The copyright holder for this preprint (which was not certified by peer review) is the author/funder, who has granted bioRxiv a license to display the preprint in perpetuity. It is made available under aCC-BY 4.0 International license.

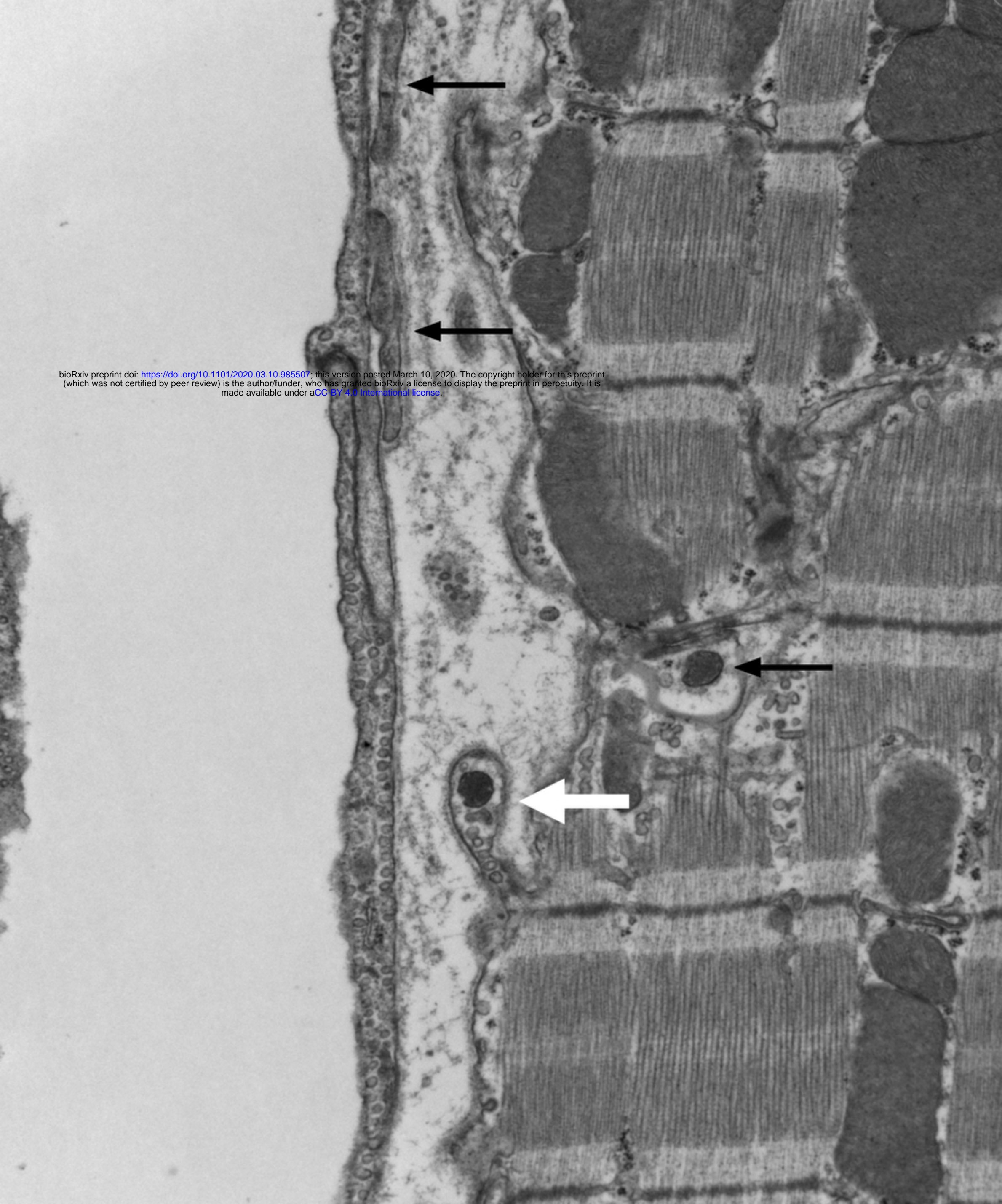


Direct Mag: 15000x
20:58:55_2019/5/16

1 μm

Figure 2

bioRxiv preprint doi: <https://doi.org/10.1101/2020.03.10.985507>; this version posted March 10, 2020. The copyright holder for this preprint (which was not certified by peer review) is the author/funder, who has granted bioRxiv a license to display the preprint in perpetuity. It is made available under aCC-BY 4.0 International license.

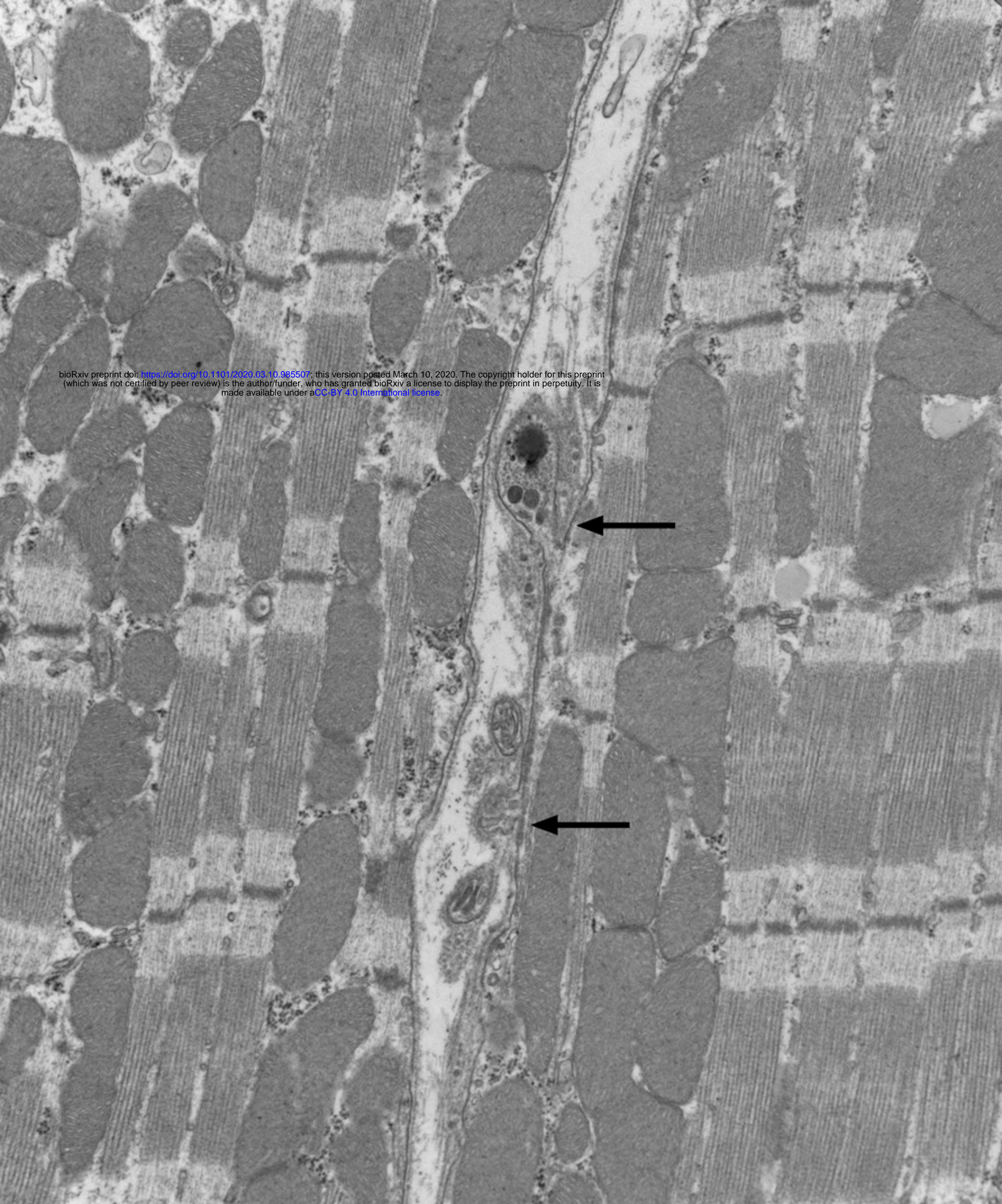


Direct Mag: 20000x
14:56:14 2019/5/9

800 nm

Figure 3

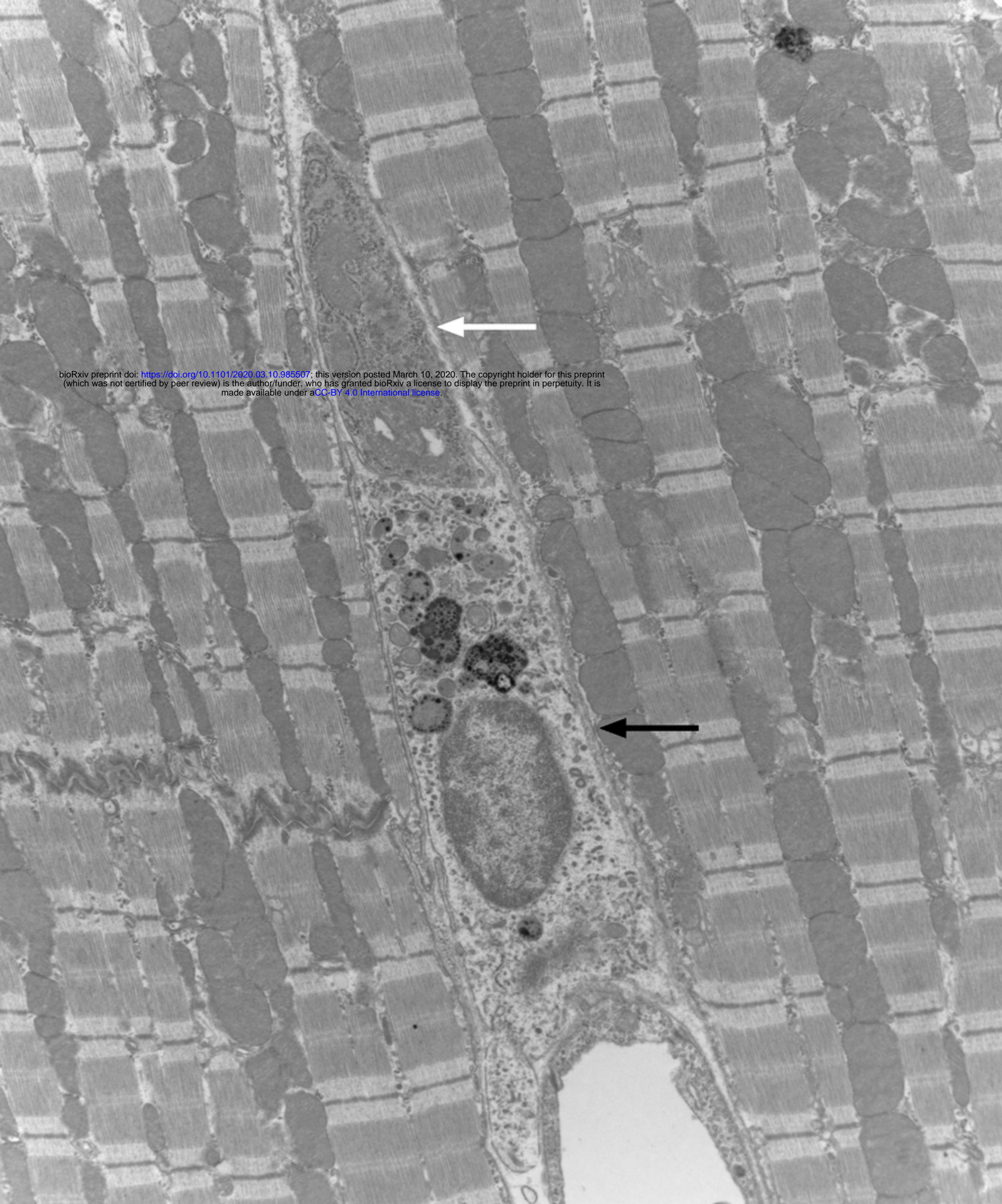
bioRxiv preprint doi: <https://doi.org/10.1101/2020.03.10.985507>; this version posted March 10, 2020. The copyright holder for this preprint (which was not certified by peer review) is the author/funder, who has granted bioRxiv a license to display the preprint in perpetuity. It is made available under aCC-BY 4.0 International license.



Direct Mag: 20000x
21:11:05 2019/5/9

800 nm

Figure 4



bioRxiv preprint doi: <https://doi.org/10.1101/2020.03.10.985507>; this version posted March 10, 2020. The copyright holder for this preprint (which was not certified by peer review) is the author/funder, who has granted bioRxiv a license to display the preprint in perpetuity. It is made available under aCC-BY 4.0 International license.

Direct Mag: 10000x
15:32:47 2019/5/9

1 μ m

Figure 5

bioRxiv preprint doi: <https://doi.org/10.1101/2020.03.10.985507>; this version posted March 10, 2020. The copyright holder for this preprint (which was not certified by peer review) is the author/funder, who has granted bioRxiv a license to display the preprint in perpetuity. It is made available under aCC-BY 4.0 International license.

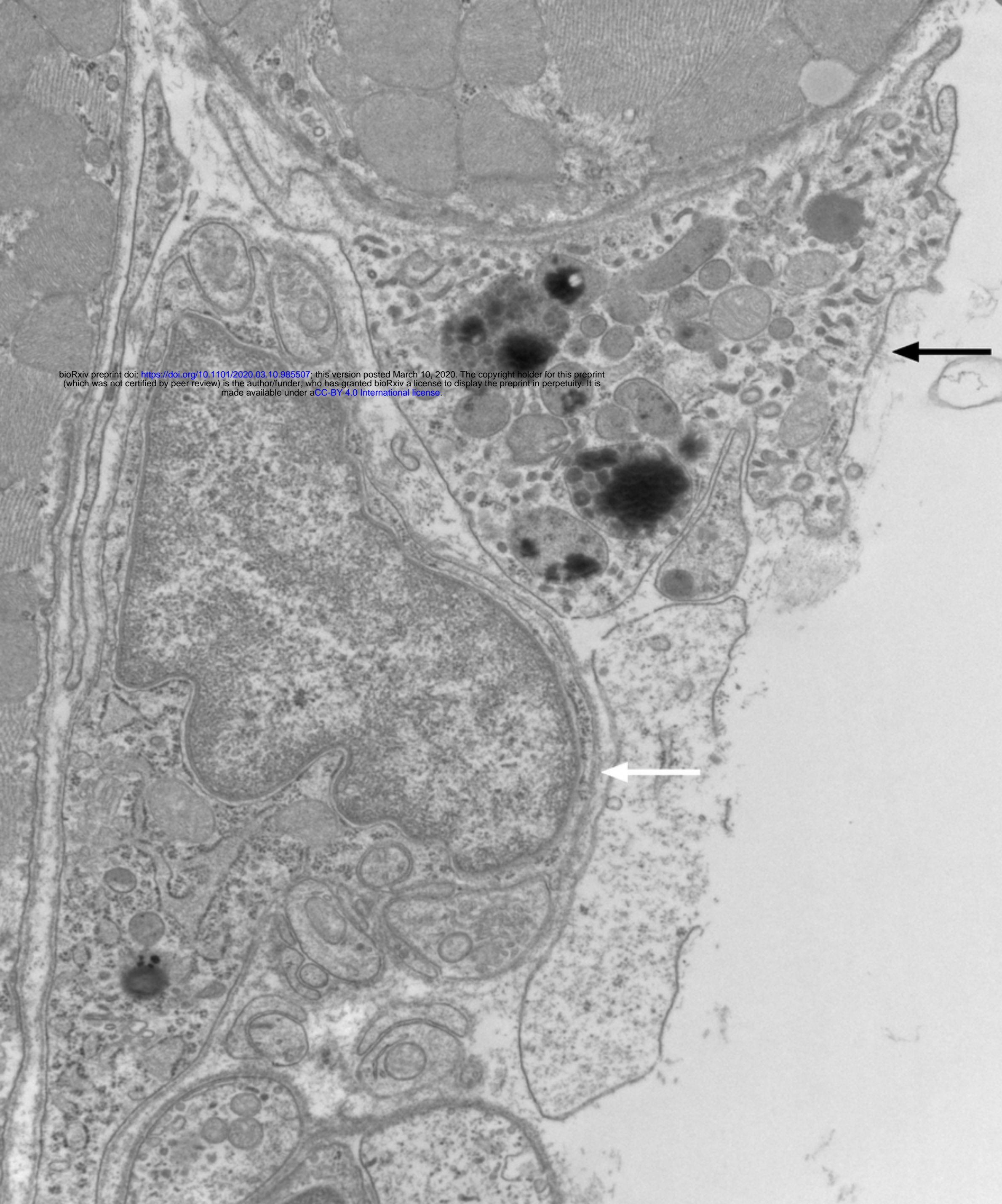


Direct Mag: 12000x
16:28:06 2019/5/9

1 μ m

Figure 6

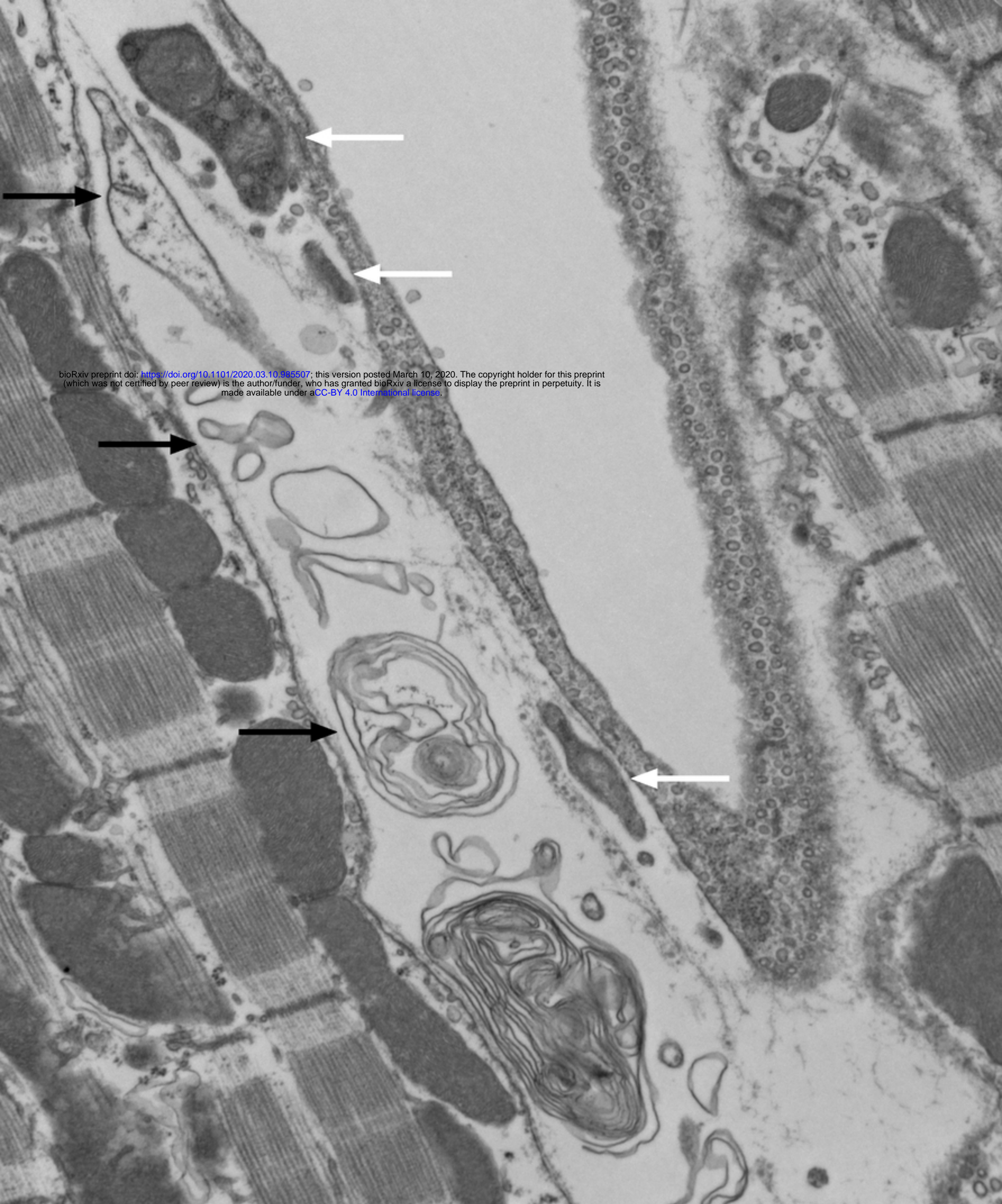
bioRxiv preprint doi: <https://doi.org/10.1101/2020.03.10.985507>; this version posted March 10, 2020. The copyright holder for this preprint (which was not certified by peer review) is the author/funder, who has granted bioRxiv a license to display the preprint in perpetuity. It is made available under aCC-BY 4.0 International license.



Direct Mag: 20000x
18:15:23 2019/5/9

800 nm

Figure 7



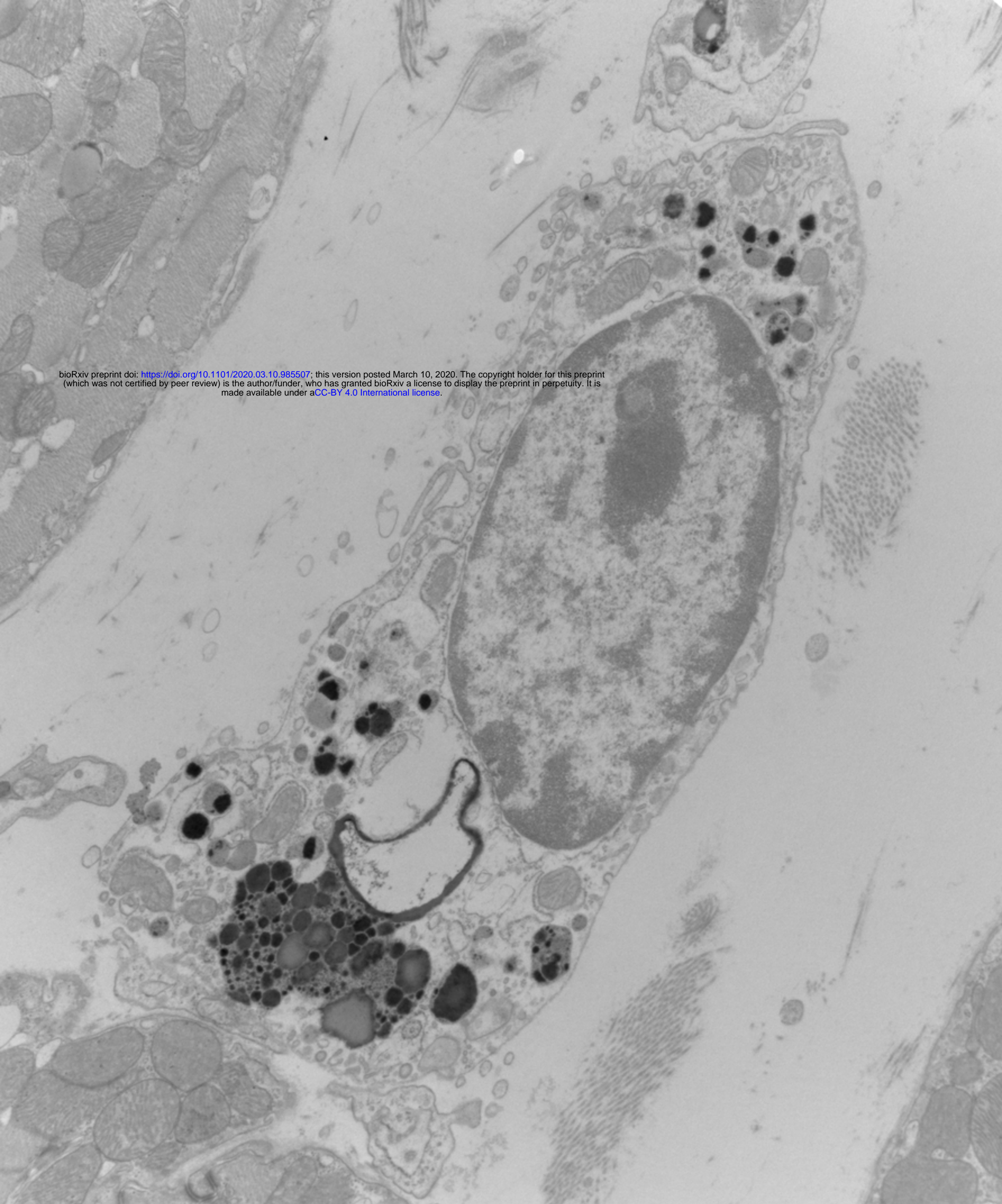
bioRxiv preprint doi: <https://doi.org/10.1101/2020.03.10.985507>; this version posted March 10, 2020. The copyright holder for this preprint (which was not certified by peer review) is the author/funder, who has granted bioRxiv a license to display the preprint in perpetuity. It is made available under aCC-BY 4.0 International license.

Direct Mag: 20000x
Caption Line 1

800 nm

Figure 8

bioRxiv preprint doi: <https://doi.org/10.1101/2020.03.10.985507>; this version posted March 10, 2020. The copyright holder for this preprint (which was not certified by peer review) is the author/funder, who has granted bioRxiv a license to display the preprint in perpetuity. It is made available under aCC-BY 4.0 International license.

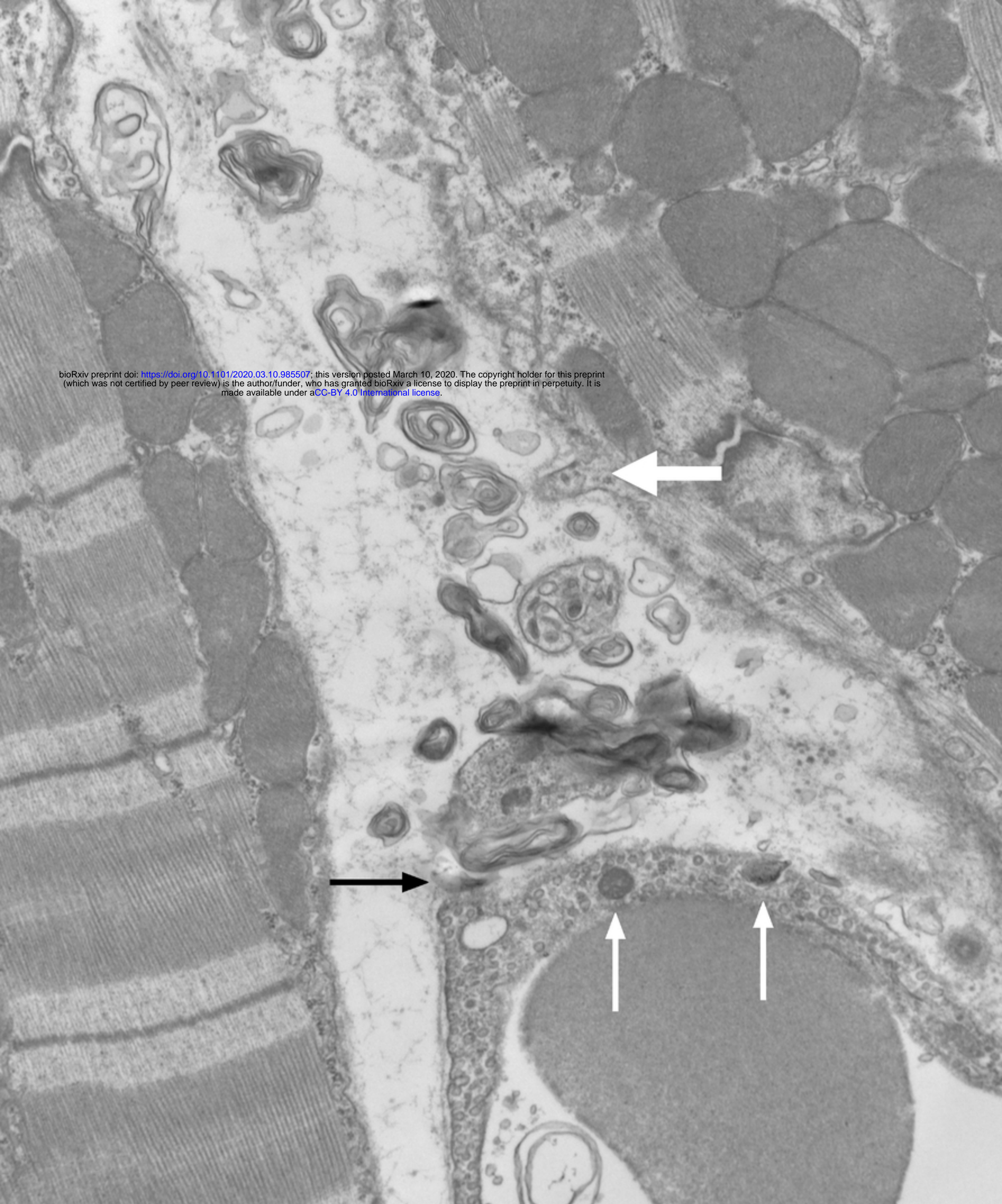


Direct Mag: 12000x
21:09:38 2019/5/16

1 μ m

Figure 9

bioRxiv preprint doi: <https://doi.org/10.1101/2020.03.10.985507>; this version posted March 10, 2020. The copyright holder for this preprint (which was not certified by peer review) is the author/funder, who has granted bioRxiv a license to display the preprint in perpetuity. It is made available under aCC-BY 4.0 International license.



Direct Mag: 20000x
11:10:46 2019/5/9

800 nm

Figure 10

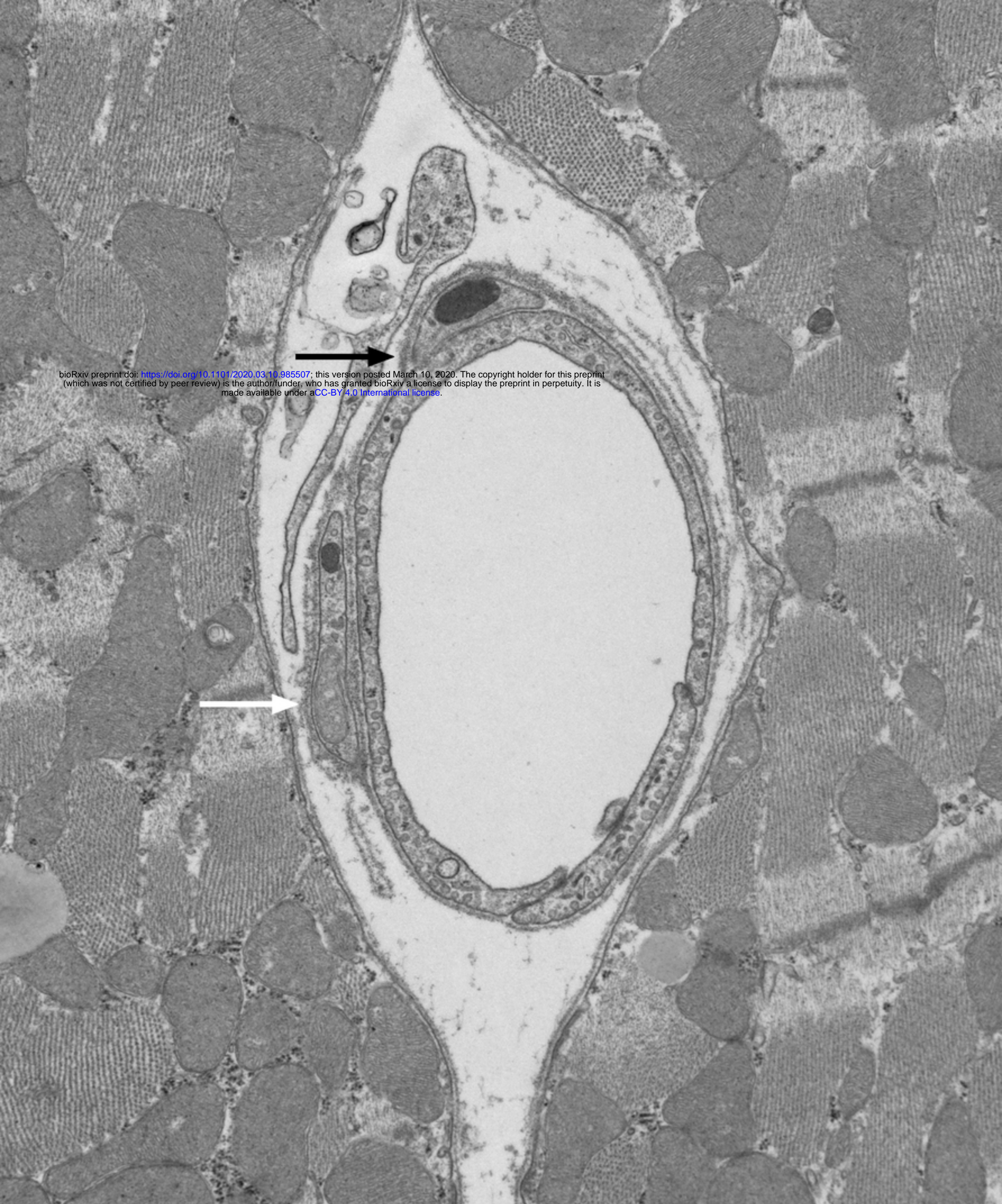
bioRxiv preprint doi: <https://doi.org/10.1101/2020.03.10.985507>; this version posted March 10, 2020. The copyright holder for this preprint (which was not certified by peer review) is the author/funder, who has granted bioRxiv a license to display the preprint in perpetuity. It is made available under aCC-BY 4.0 International license.



Direct Mag: 20000x
15:08:21 2019/5/9

800 nm

Figure 11



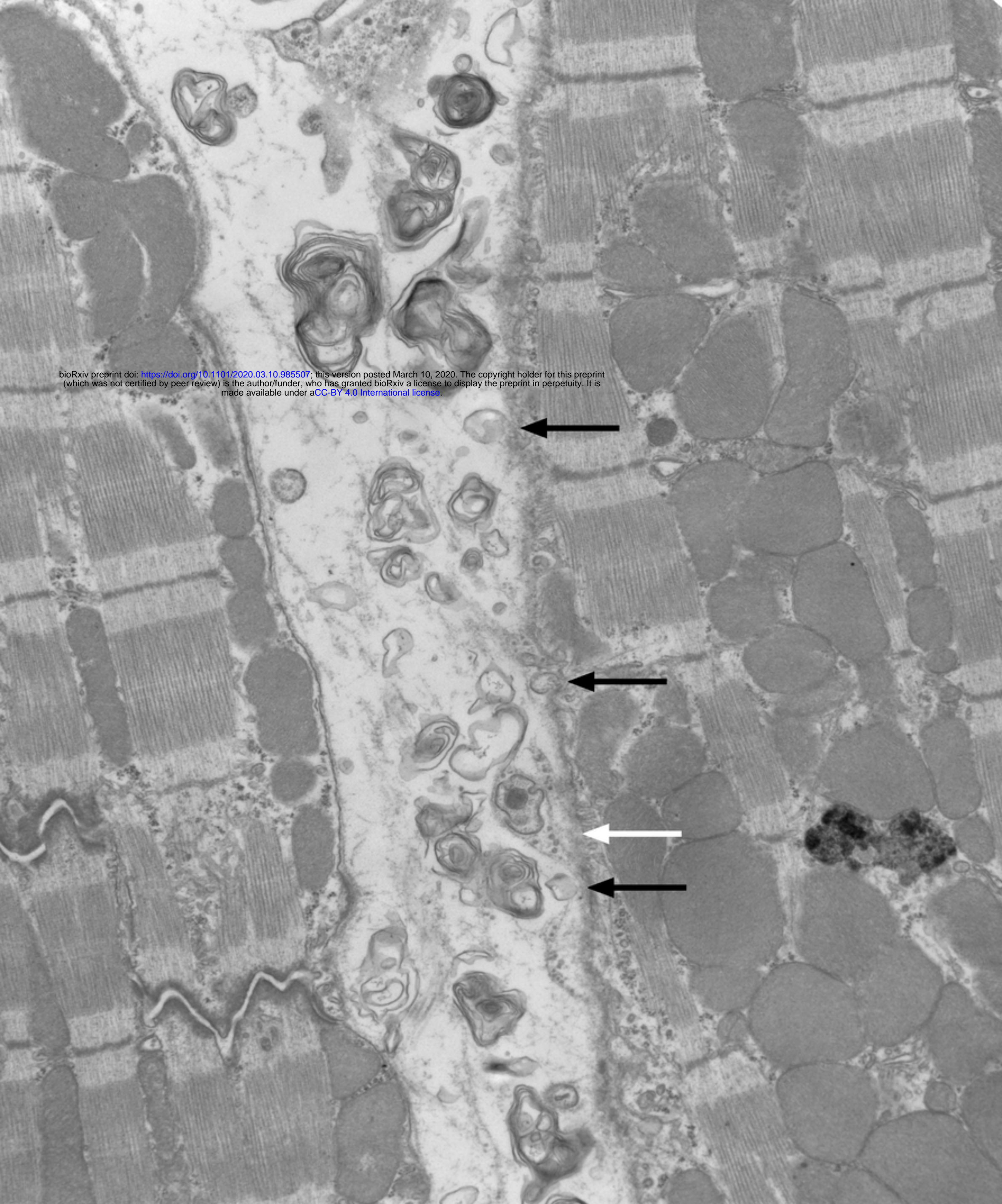
bioRxiv preprint doi: <https://doi.org/10.1101/2020.03.10.985507>; this version posted March 10, 2020. The copyright holder for this preprint (which was not certified by peer review) is the author/funder, who has granted bioRxiv a license to display the preprint in perpetuity. It is made available under aCC-BY 4.0 International license.

Direct Mag: 20000x
22:13:56 2019/5/9

800 nm

Figure 12

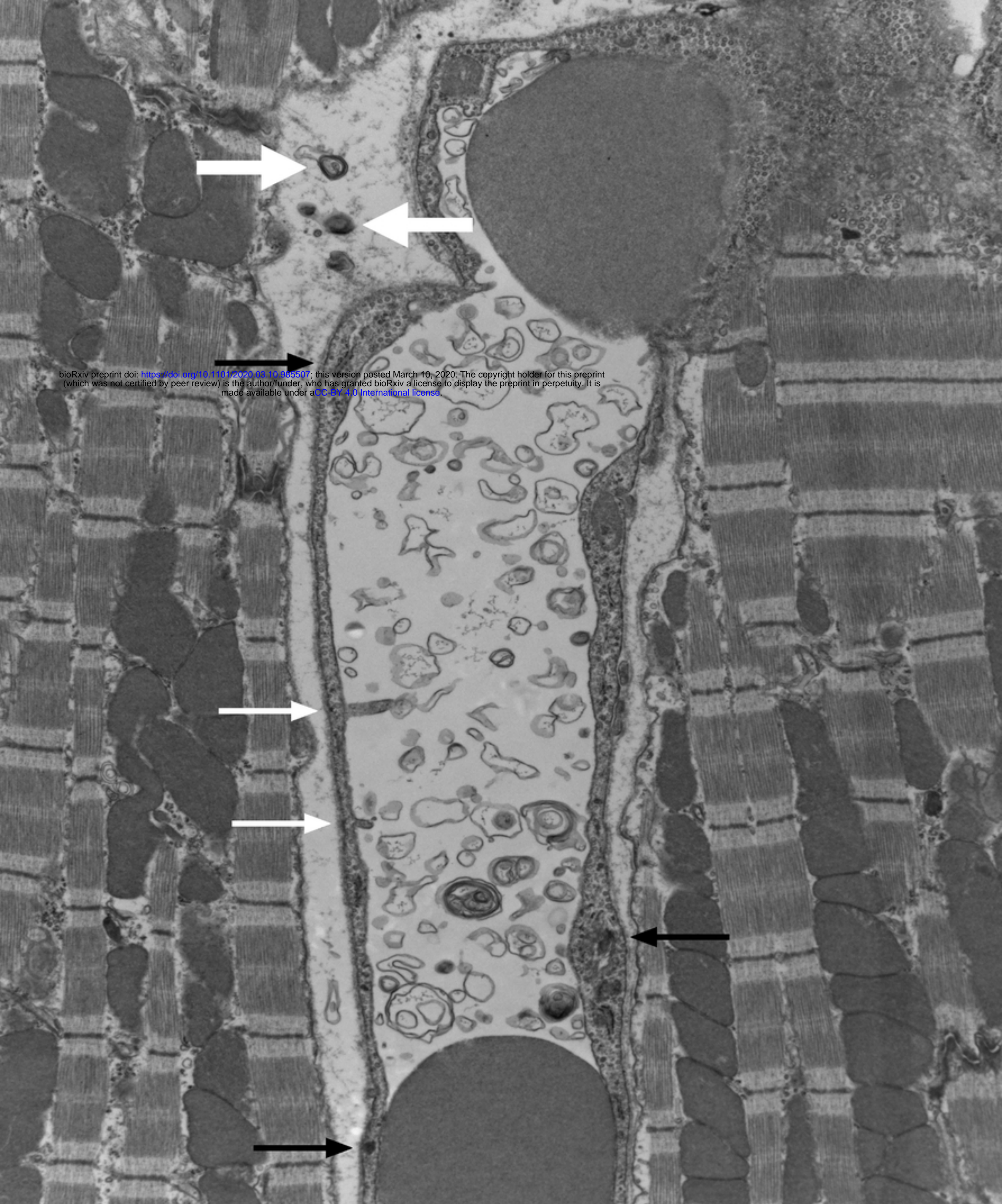
bioRxiv preprint doi: <https://doi.org/10.1101/2020.03.10.985507>; this version posted March 10, 2020. The copyright holder for this preprint (which was not certified by peer review) is the author/funder, who has granted bioRxiv a license to display the preprint in perpetuity. It is made available under aCC-BY 4.0 International license.



Direct Mag: 20000x
15:20:20 2019/5/9

800 nm

Figure 13



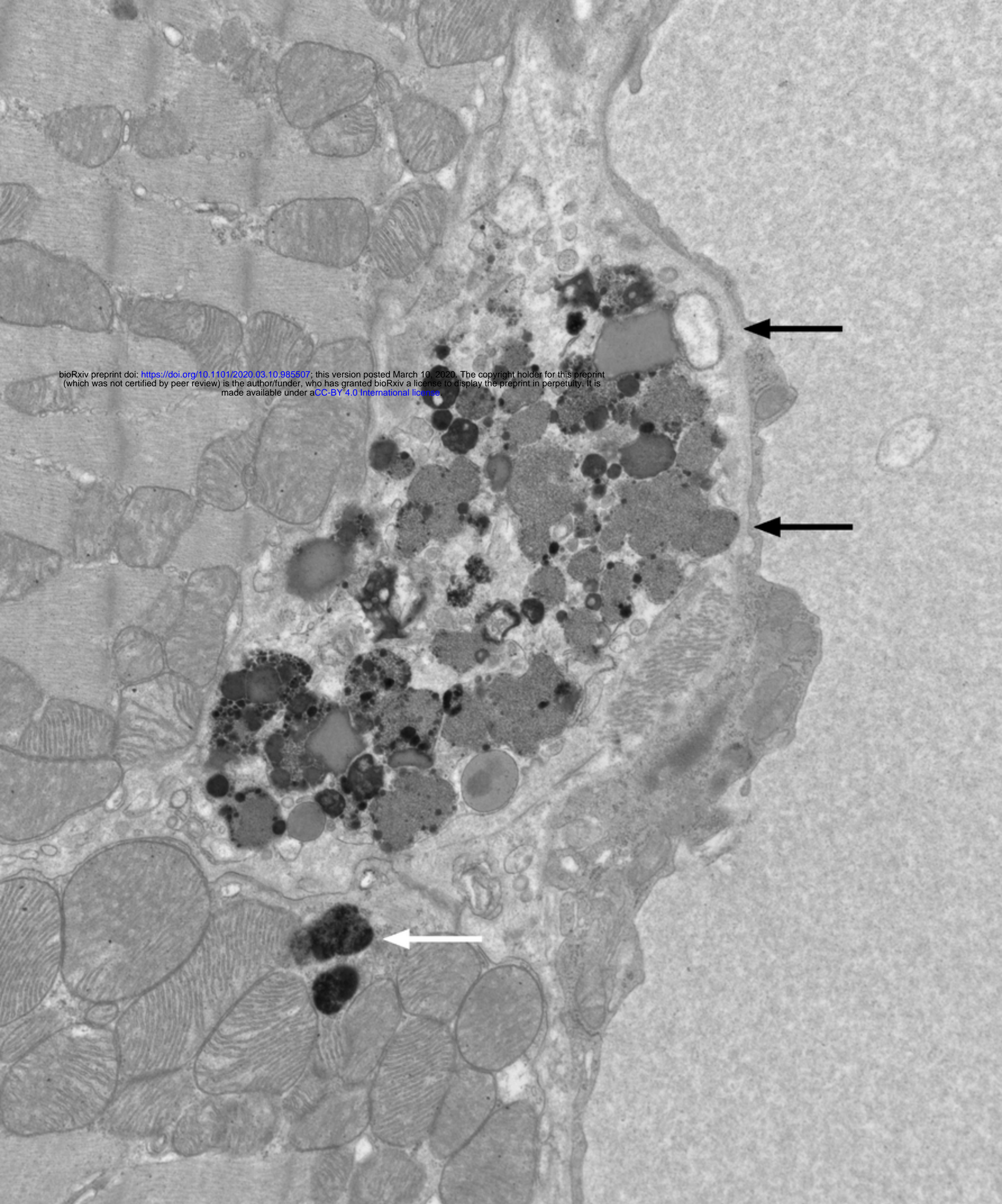
bioRxiv preprint doi: <https://doi.org/10.1101/2020.03.10.985507>; this version posted March 10, 2020. The copyright holder for this preprint (which was not certified by peer review) is the author/funder, who has granted bioRxiv a license to display the preprint in perpetuity. It is made available under aCC-BY 4.0 International license.

Direct Mag: 10000x
15:54:18_2019/5/9

1 μm

Figure 14

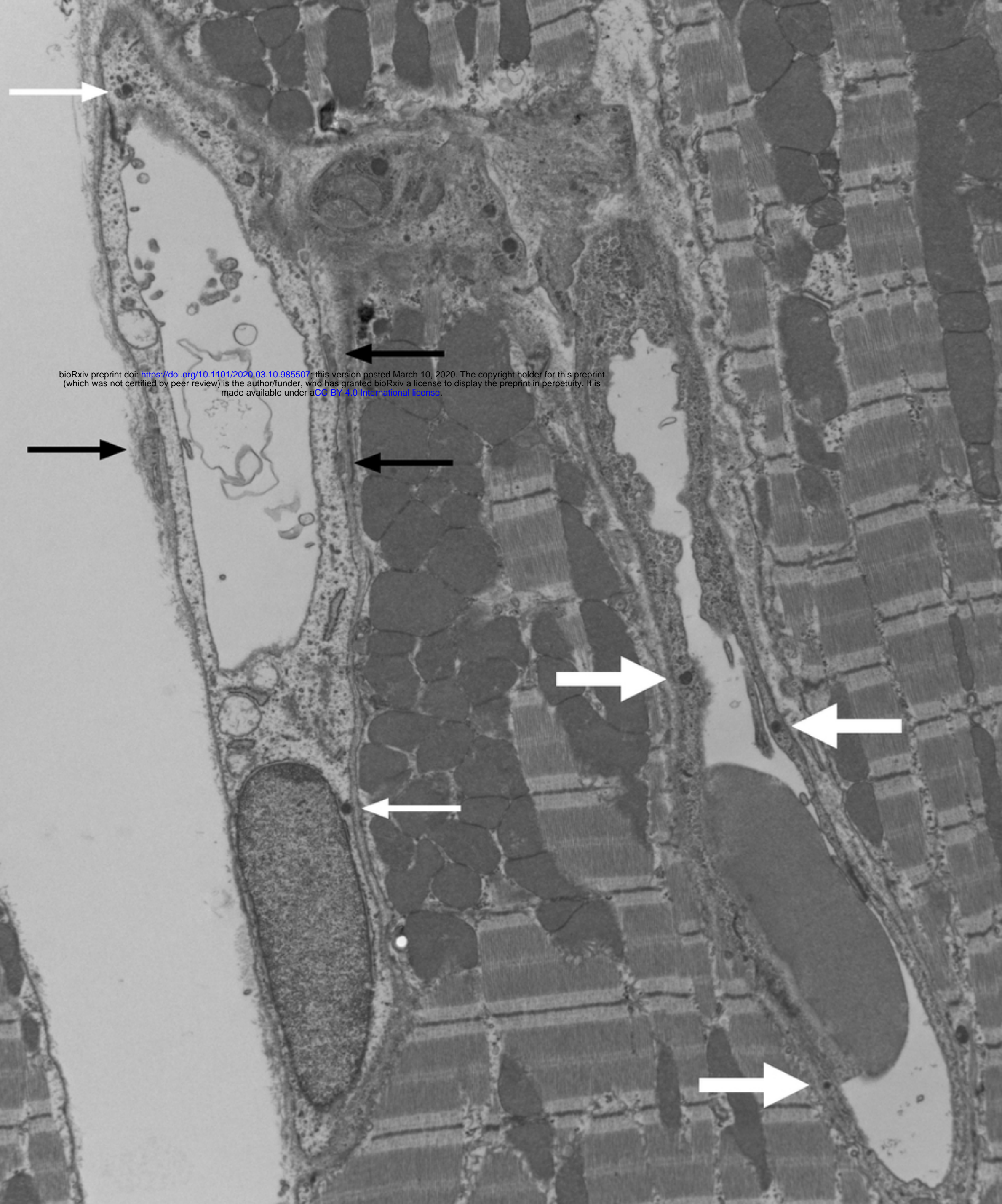
bioRxiv preprint doi: <https://doi.org/10.1101/2020.03.10.985507>; this version posted March 10, 2020. The copyright holder for this preprint (which was not certified by peer review) is the author/funder, who has granted bioRxiv a license to display the preprint in perpetuity. It is made available under aCC-BY 4.0 International license.



Direct Mag: 15000x
21:18:18 2019/5/16

1 μ m

Figure 15



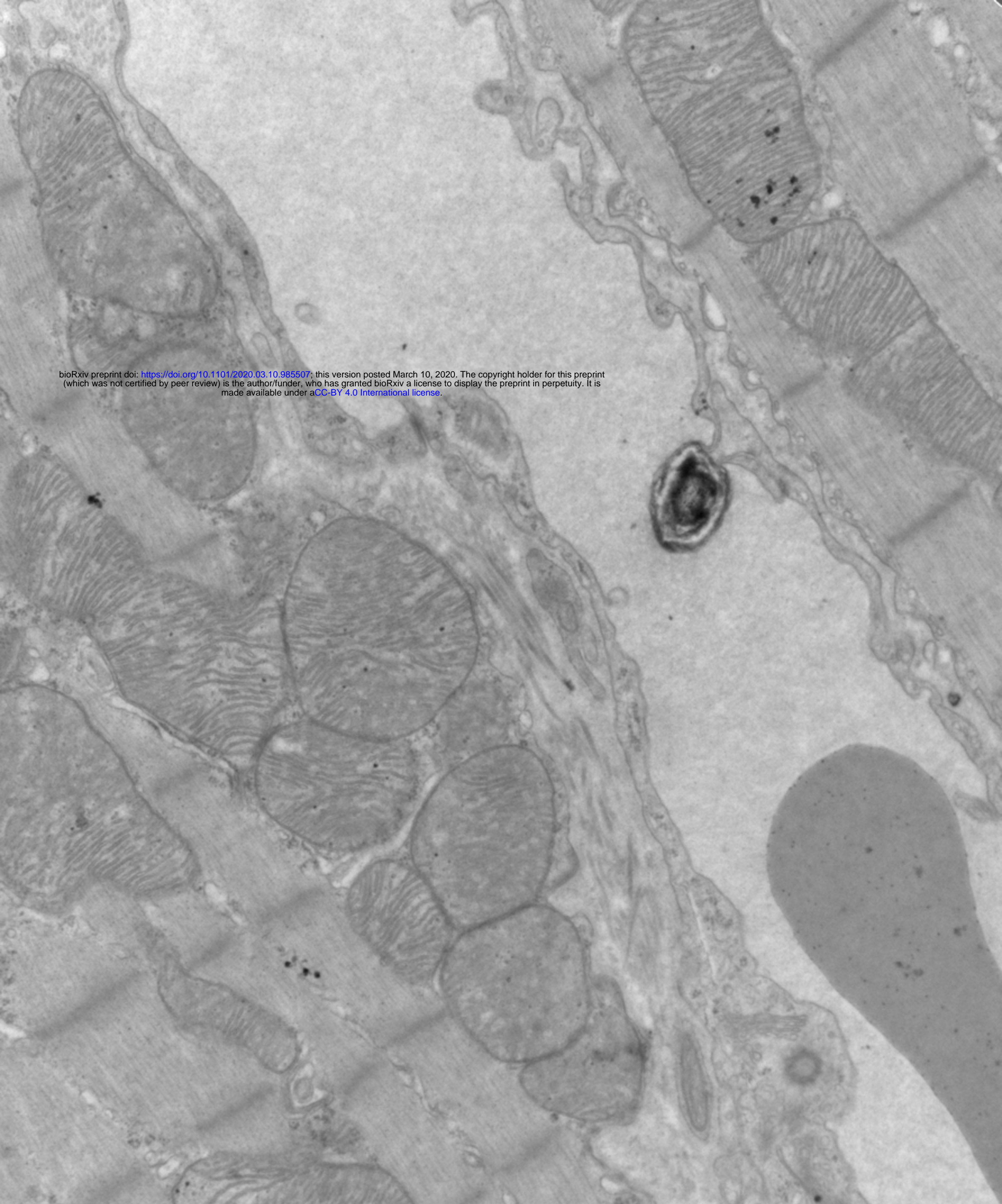
bioRxiv preprint doi: <https://doi.org/10.1101/2020.03.10.985507>; this version posted March 10, 2020. The copyright holder for this preprint (which was not certified by peer review) is the author/funder, who has granted bioRxiv a license to display the preprint in perpetuity. It is made available under aCC-BY 4.0 International license.

Direct Mag: 8000x
15:35:50 2019/5/9

2 μ m

Figure 16

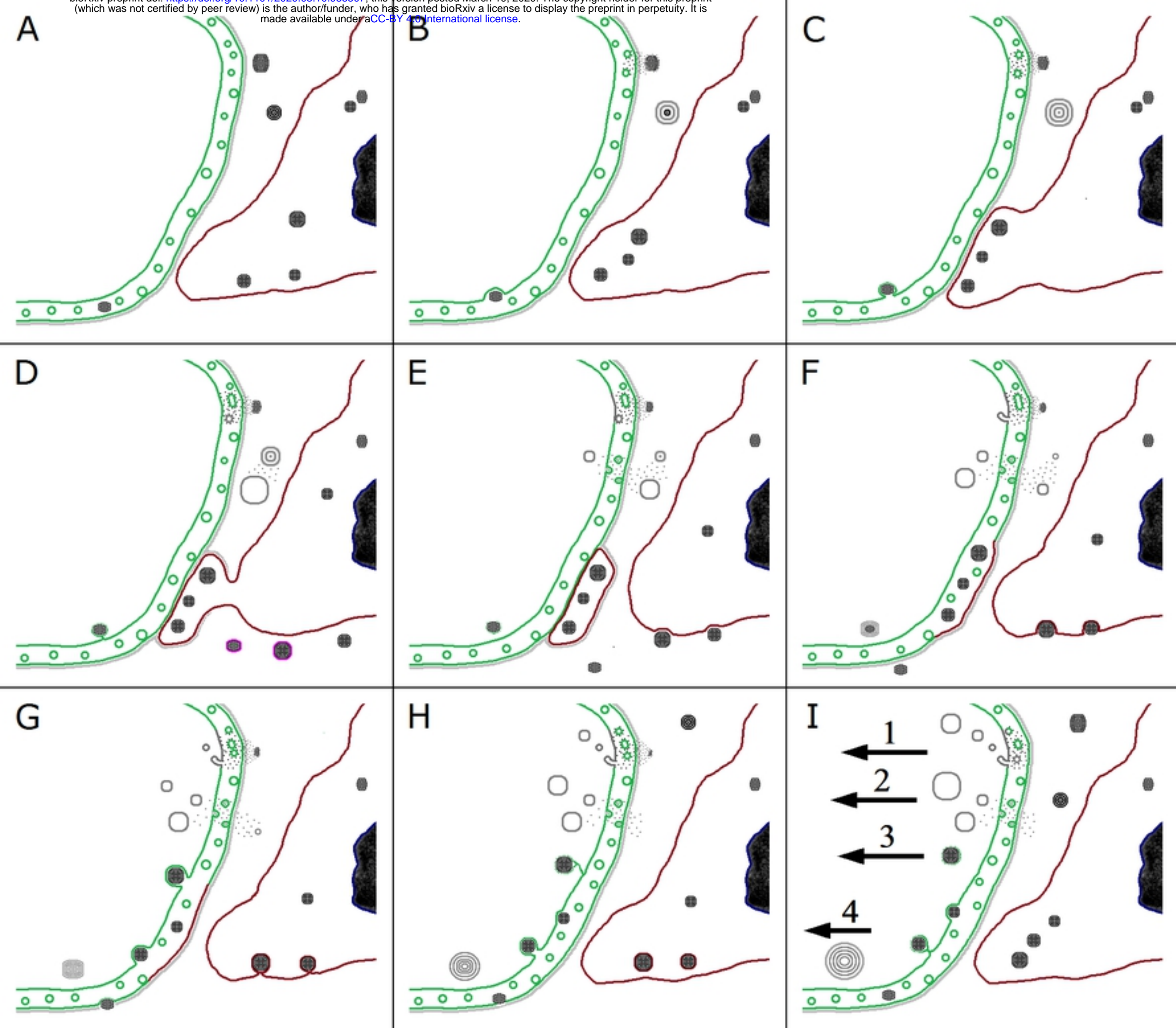
bioRxiv preprint doi: <https://doi.org/10.1101/2020.03.10.985507>; this version posted March 10, 2020. The copyright holder for this preprint (which was not certified by peer review) is the author/funder, who has granted bioRxiv a license to display the preprint in perpetuity. It is made available under aCC-BY 4.0 International license.



Direct Mag: 20000x
20:16:03 2019/5/16

800 nm

Figure 17



Figure